Molecular Therapy
Methods & Clinical Development
Original Article

Accelerating clinical-scale production of BCMA CAR T cells with defined maturation stages

Jara J. Joedicke,[1] Ulrich Großkinsky,[1] Kerstin Gerlach,[1] Annette Künkele,[2,3] Uta E. Höpken,[4] and Armin Rehm[1]

[1]Department of Translational Tumorimmunology, Max-Delbrück-Center for Molecular Medicine, 13125 Berlin, Germany; [2]Charité-University Medicine, Berlin, Corporate Member of Freie Universität Berlin and Humboldt-Universität zu Berlin, Department of Pediatric Oncology and Hematology, 13353 Berlin, Germany; [3]Charité-University Medicine, Berlin, Corporate Member of Freie Universität Berlin and Humboldt-Universität zu Berlin, Stem Cell Facility, Department of Hematology, Oncology and Tumorimmunology, 13353 Berlin, Germany; [4]Department of Microenvironmental Regulation in Autoimmunity and Cancer, Max-Delbrück-Center for Molecular Medicine, 13125 Berlin, Germany

The advent of CAR T cells targeting CD19 or BCMA on B cell neoplasm demonstrated remarkable efficacy, but rapid relapses and primary refractoriness remains challenging. A leading cause of CAR T cell failure is their lack of expansion and limited persistence. Long-lived, self-renewing multipotent T memory stem cells (T_{SCM}) and T central memory cells (T_{CM}) likely sustain superior tumor regression, but their low frequencies in blood from cancer patients impose a major hurdle for clinical CAR T production. We designed a clinically compliant protocol for generating BCMA CAR T cells starting with increased T_{SCM}/T_{CM} cell input. A CliniMACS Prodigy process was combined with flow cytometry-based enrichment of $CD62L^+CD95^+$ T cells. Although starting with only 15% of standard T cell input, the selected T_{SCM}/T_{CM} material was efficiently activated and transduced with a BCMA CAR-encoding retrovirus. Cultivation in the presence of IL-7/IL-15 enabled the harvest of CAR T cells containing an increased $CD4^+$ T_{SCM} fraction and 70% T_{SCM} cells amongst $CD8^+$. Strong cell proliferation yielded cell numbers sufficient for clinical application, while effector functions were maintained. Together, adaptation of a standard CliniMACS Prodigy protocol to low input numbers resulted in efficient retroviral transduction with a high CAR T cell yield.

INTRODUCTION

The clinical application of second-generation chimeric antigen receptor (CAR) T cells targeted at the CD19 antigen on B cell neoplasm has shown remarkable response rates ranging from 50% to 85% depending on the B cell malignancy, followed by extended disease-free and overall survival rates.[1–4] The second most frequently targeted antigen is the B cell maturation antigen (BCMA), which is broadly expressed in multiple myeloma. Clinical trials demonstrated high response rates of BCMA CAR T cells as well, but median progression-free survival was shorter than for CD19 CAR T cells.[5,6] Frequent relapses in CD19 and BCMA CAR T cell-treated patients, in conjunction with the failure to achieve complete remissions, point to the medical need to improve the efficacy of this innovative technology.[7] One main reason for CAR treatment failure is that CAR T cell expansion immediately after infusion ceases, and long-term persistence despite initial tumor control is insufficient.[8]

To overcome the weakness of low CAR T cell fitness and proliferative capacity, these properties inherent to current manufacturing protocols can be avoided by enriching early memory CAR T cell subsets. Although in adoptive transfer T effector memory cells (T_{EM}) undergo apoptosis earlier and persist only for a short time span, T central memory cells (T_{CM}) and T stem cell memory cells (T_{SCM}) have been suggested as differentiation stages that endow CAR- and TCR-modified T cells with longer persistence.[9–13] Notably, the frequency of T_{SCM} in the manufactured products was found to be positively correlated with CAR T cell expansion *in vivo*, and this feature might even be a positive biomarker for anti-tumor efficacy.[7] A high degree of variability in T cell differentiation states among patients exists, which may strongly influence the final product composition.[14] These variabilities are influenced by inherent properties of the patient, but most likely disease histology, prior treatments, and age determine the fitness of the T cell population.

To date, the only approved CAR T products are generated from autologous donors, their subset and differentiation heterogeneity makes the application of a standardized protocol for Good Manufacturing Practice (GMP)-compliant manufacturing desirable for several reasons. First, it has been suggested that innovative protocols can overcome initial T cell defects and result in T_{SCM}-enriched CAR T cell products that are qualitatively more similar to the ones generated from healthy donors.[7] Second, from a scientific view, starting with well-defined T_{SCM} and T_{CM} make CAR T cell protocols more

Received 2 April 2021; accepted 22 December 2021;
https://doi.org/10.1016/j.omtm.2021.12.005.

Correspondence: Armin Rehm, MD, Department of Translational Tumorimmunology, Max-Delbrück-Center for Molecular Medicine, Robert-Rössle-Straße 10, 13125 Berlin, Germany.
E-mail: arehm@mdc-berlin.de
Correspondence: Uta E. Höpken, PhD, Department of Microenvironmental Regulation in Autoimmunity and Cancer, Max-Delbrück-Center for Molecular Medicine, Robert-Rössle-Straße 10, 13125 Berlin, Germany.
E-mail: uhoepken@mdc-berlin.de

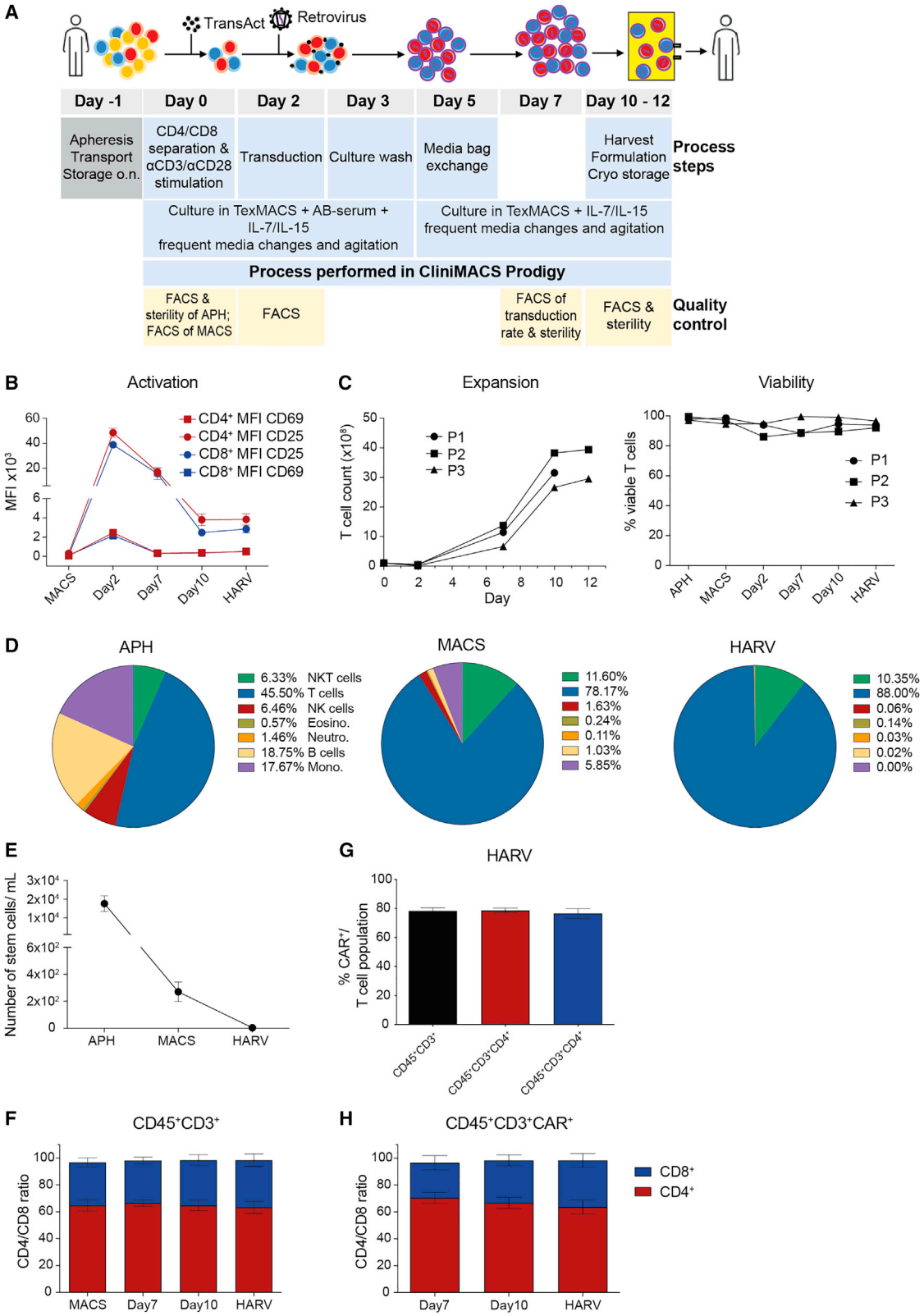

(legend on next page)

comparable regarding cell culture conditions, retro- or lentiviral transduction, modular composition of CARs, costimulatory domains, cytokine stimulation, and other crucial properties.

A bottleneck of T_{SCM} enrichment is their paucity in peripheral blood from patients pretreated with myelosuppressive chemotherapies.[8] In general, CAR T cell manufacturing involves multiple handling steps, including separation, stimulation, transduction, and long-term cultivation.[15] Protocols that additionally require T cell subset separation cannot be consistently performed in a fully closed systems. For example, previous protocols for the enrichment of T_{SCM} and T_{CM} use sequential steps of streptamer-coated magnetic microbeads.[9,11,16]

The CliniMACS Prodigy system (also referred to as Prodigy) has gained considerable attention for the clinical enrichment of CAR T cell products within a fully closed system. It has been mostly used for the production of lentivirally transduced CAR T cells.[7,14,15,17–25] To our knowledge, studies of γ-retrovirally transduced CAR T cells in the Prodigy are missing, although γ-retroviruses have attractive biological and economic features that make them suitable for clinical applications. For example, they have an acceptable oncogenic and genotoxic risk profile, their production on a clinical scale is economic and affordable for academic institutions, and they have proven efficiency and consistency in CD19 CAR T cell trials, as seen for the approved product axicabtagene ciloleucel (Yescarta).[26,27]

To simplify and accelerate the standardization of T_{SCM}- and T_{CM}-dependent BCMA CAR T cell generation, we here combined a two-step T_{SCM} and T_{CM} enrichment protocol with the closed GMP-compatible Prodigy process. A magnetic-activated cell sorting (MACS)-bead enrichment of $CD4^+$ and $CD8^+$ T cells performed on the Prodigy was followed by an aseptic flow cytometry sorting step to further select for a $CD95^+CD62L^+$ T cell population that was enriched for T_{CM} and T_{SCM}. Following reinsertion into the closed Prodigy system, we proved that the activation matrix can be adapted to the needs of very low T cell input material and that the γ-retroviral transduction process is compatible with the Prodigy process. Activation and transduction of sorted T cells in the presence of interleukin (IL)-7 and IL-15 resulted in the generation of a larger fraction of T_{SCM}-like cells, which displayed phenotypic features of naturally developing T_{SCM}. The yield of BCMA CAR-transduced T cells fulfilled the release criteria after 10–12 days, thus demonstrating the feasibility to start with a small amount of a defined T cell subset and yet to manufacture a clinical-scale product in a partly automated and closed system.

RESULTS

Automated TCT process using the CliniMACS Prodigy leads to high BCMA CAR T cell transduction rates and cell yield

To produce clinically relevant numbers of BCMA CAR T cells,[28] the Prodigy platform was chosen. This instrument integrates magnetic bead cell separation and bioreactor functions in a closed system, accessible by sterile tube welding. Leukapheresis material was used within 24 h of donation, and cells were adjusted to an appropriate dilution and then applied to the tubing set TS520 installed on the Prodigy. In our T cell transduction (TCT) protocol, T cells were initially enriched for $CD4^+$ and $CD8^+$ and then activated using α-CD3/α-CD28 coated TransAct beads (Figure 1A). As input material, 1×10^8 T cells ($CD45^+CD3^+$7-AAD^-) were seeded. An activity matrix that was different from the manufacturer's recommendations for the usage of lentivirus was programmed to control for the stepwise execution of retroviral transduction (day 2), culture wash, medium exchange volume and timing, volume adjustment, and shaker activity (Table S1). The cells were expanded until days 10–12 and then cryopreserved for later analysis. For the first 5 days, TexMACS medium supplemented with 1% human AB serum and the cytokines IL-7 and IL-15 (medium 1) were used. After that, serum was gradually reduced by medium exchanges with serum-free TexMACS (medium 2, only IL-7 and IL-15) (Figure 1A). Microbial contamination was excluded by an aerobic and anaerobic BACTEC test. In all process steps, the results for the microbiological control were negative. We conclude that our process established on the Prodigy platform is

Figure 1. A clinical-scale γ-retroviral transduction procedure for the generation of BCMA CAR T cells results in high transduction and expansion rates

(A) Graphical representation of the BCMA CAR T cell production process in the CliniMACS Prodigy. CD4/CD8 T cells are magnetically separated in the CliniMACS Prodigy (light blue boxes) and subsequently stimulated with α-CD3/α-CD28 coated TransAct beads. Cells were cultured in TexMACS medium supplemented with 1% human AB serum, 12.5 ng/mL IL-7, and 12.5 ng/mL IL-15. Retroviral transduction with an MOI of 2 was performed on day 2, followed by a culture wash on day 3. Serum-free medium was used from day 5 on. The final product was harvested between days 10 and 12 of culture. Culture conditions, sterility, and cell phenotype were analyzed during the whole process (yellow boxes). (B) Flow cytometric analysis of the activation profile, as determined by the expression of CD25 and CD69 on viable 7-$AAD^-CD45^+CD3^+$ T cells. Values represent mean fluorescence intensity (MFI) subtracted by a fluorescence minus 1 (FMO) sample. (C) Total numbers of $CD3^+$ T cells (left) and their viability (7-AAD^-) (right). (D) Cellular composition at different process steps, as determined by staining with leukocyte subset specific markers, was done as follows: NKT cells, 7-$AAD^-CD45^+CD3^+CD16^+/CD56^+$; T cells, 7-$AAD^-CD45^+CD3^+CD16^-/CD56^-$, additionally $CD4^+CD8^-$ T cells and $CD8^+CD4^-$ T cells; NK cells, 7-AAD^-CD45^+-$CD3^-CD14^-CD19^-$SSC-$A^{low}CD16^+/CD56^+$; eosinophils, 7-$AAD^-CD45^+CD3^-CD14^-CD19^-$SSC-$A^{high}CD16^-/CD56^-$; neutrophils, 7-$AAD^-CD45^+$-$CD3^-CD14^-CD19^-$SSC-$A^{high}CD16^+/CD56^+$; B cells, 7-$AAD^-CD45^+CD3^-CD14^-CD19^+$; monocytes, 7-$AAD^-CD45^+CD3^-CD14^+CD19^-$; CD16 and CD56 were stained in the same channel. APH, apheresis material; MACS, magnetically separated $CD4^+/CD8^+$ T cells; HARV, final product after formulation. The pie chart represents the mean of n = 3 Prodigy runs. (E) Quantitation of stem cells (debri$^-CD45^+$7-AAD^-SSC-$A^{low}CD34^+$) in the initial apheresis (APH) sample, MACS-purified fraction (MACS), and final product (HARV). (F) Ratio of $CD4^+$ and $CD8^+$ viable 7-$AAD^-CD45^+CD3^+$ T cells in the whole culture. (G) Frequencies of CAR^+ T cells among all T cells (7-$AAD^-CD45^+CD3^+$) and in $CD4^+$ and $CD8^+$ T cell subpopulations of the final product (HARV) were determined. (H) Frequencies of $CD4^+$ and $CD8^+$ T cells within the CAR^+ fraction at different process steps (MACS, day 7, day 10, and HARV) were determined. All samples were run in technical duplicates, and results are displayed as mean only (D) or mean ± SEM (B, C, and D–G). Data are for n = 3 independent Prodigy runs.

Table 1. Quantification of process efficiency using bulk T cells as input material in P1–P3

Run	Starting Cell No.	Process Duration	CD4/CD8 Ratio in HARV	Expansion Rate[a]	T Cell No. in HARV	Transduction Rate of $CD45^+CD3^+$ in HARV	CAR T Cell No. in HARV	VCN
P1	1×10^8	10 days	71.2%/26.7%	59×	3.17×10^9	72.15%	2.29×10^9	2.6
P2	1×10^8	12 days	70.1%/29.5%	85×	4.11×10^9	82.95%	3.41×10^9	3.2
P3	1×10^8	12 days	48.5%/49.5%	188×	3.08×10^9	80.10%	2.46×10^9	3.4

[a]The expansion rate was calculated from day 2 on.

GMP compliant and can be properly controlled in all critical handling steps.

To explore the efficiency of retroviral transduction, TransAct bead-stimulated CD4 and CD8 T cells were transduced by spinoculation with addition of the transduction enhancer Vectofusin-1 on day 2. A SIN vector-based BCMA CAR γ-retrovirus at an MOI of 2 was applied. Increased CD69 and CD25 expression indicated a T cell activation peak (Figure 1B). As observed also by others,[21] T cell numbers after 2 days of activation declined more than half (day 0, input cell number 1×10^8; day 2, 0.16×10^8 to 0.54×10^8). Expansion rates between day 2 and harvest were 59-, 85-, and 188-fold (Table 1). Cultivation was terminated when $>2 \times 10^9$ T cells were obtained. Over the cultivation period of 10 or 12 days, T cells expanded rapidly to clinically relevant numbers of viable $CD45^+CD3^+CAR^+$7-AAD^- CAR^+ T cells (2.29×10^9 to 3.41×10^9) (Figure 1C; Table 1).

Magnetic separation of $CD4^+$ and $CD8^+$ T cells led to an enrichment of $CD45^+CD3^+CD16^-CD56^-$ T cells from 45.50% (±4.63% SEM) in the apheresis starting material (APH) to 78.17% (±4.64% SEM) in the MACS fraction. In the harvested product (HARV), strongly enriched populations of 88.00% (±0.65% SEM) T cells and 10.35% (±0.54% SEM) NKT cells ($CD45^+CD3^+CD16^+CD56^+$) were recovered (Figures 1D and S1A). An important safety measure is the determination of residual hematopoietic stem cells, as this cell population is more susceptible to retrovirus-induced malignant transformation.[29,30] Stem cell frequencies, defined as $CD45^{int}CD34^+$7-AAD^- and gated according to the International Society of Hematotherapy and Graft Engineering (ISHAGE) guidelines[31,32] (Figure S1B), decreased to undetectable numbers in the final product (HARV) (Figure 1E).

The CD4/CD8 T cell ratios showed a predominance of CD4 T cells (CD4/CD8 ratio about 65%:35%) in the MACS-enriched input material, which was maintained over the whole cultivation phase (Figure 1F). T cell transduction rates between 72% and 83% were achieved, while the vector copy number (VCN) per transduced T cell remained between 2.6 and 3.4 retroviral copies, thus representing an acceptable risk profile (Figure 1G; Table 1). In the CAR^+ T cell population, a modest shift of the CD4/CD8 ratio from day 7 to the harvested product toward $CD8^+$ T cells (Figure 1H) was obtained. In summary, γ-retroviral transduction in an automated bioreactor system yielded efficient retroviral transduction and expansion rates of BCMA CAR T cells.

BCMA CAR T cells show efficient target cell killing and cytokine release *in vitro*

To determine the functional capacity of BCMA CAR T cells produced on a clinical scale, a chromium release assay was performed. BCMA CAR T cells were co-cultured with [^{51}Cr]-labeled $BCMA^{high}$ multiple myeloma target cell lines, NCI-H929 and OPM-2, resulting in an efficient cytolytic activity at different effector to target ratios; $BCMA^-$ REH B-acute lymphoblastic leukemia (B-ALL) cells were not killed (Figure 2A). Killing of $BCMA^{high}$ multiple myeloma cell lines positively correlated with BCMA surface expression (Figure 2B).

To further assess the antigen specificity and effector capacity of BCMA CAR T cells, they were co-cultured with $BCMA^{low}$-expressing B-NHL target cell lines. In the presence of JeKo-1 (mantle cell lymphoma [MCL]) and DOHH-2 (diffuse large B cell lymphoma [DLBCL]) cell lines, BCMA CAR T cells released profound amounts of IFN-γ, IL-2, and TNF-α; they produced only background cytokine levels when challenged with $BCMA^-$ REH cells (Figure 2C). For these $BCMA^{low}$-expressing B-NHL cell lines, a correlation of BCMA surface density with effector cytokine release was not found (Figure 2D). Together, clinical-scale BCMA CAR T cell production endowed T cells with CAR-dependent effector functions. Considering all analytical results, the essential acceptance criteria regarding purity, quantity, safety, and potency were met.

Development of a Prodigy process using T_{CM} and T_{SCM} cells as starting material for BCMA CAR T cell production

In runs P1, P2, and P3, here referred to as bulk runs, cell harvest yielded high frequencies of T_{CM} ($CD3^+CD95^+CD62L^+CD45RO^+$) in the $CD4^+$ (96.87% ± 1.06% SEM) and $CD8^+$ (82.02% ± 3.28% SEM) compartment (Figure 3A). On the other hand, only minor amounts of T_{SCM} cells ($CD3^+CD95^+CD62L^+CD45RO^-$) were generated, which were found mostly in the $CD8^+$ T cell compartment (9.46% ± 3.36% SEM) compared with $CD4^+$ T cells (0.26% ± 0.06% SEM) (Figures 3A and S2A).

To facilitate a broader application of T_{CM} and T_{SCM} for CAR T cell production, avoiding further pharmacological interference with T cell maturation,[9,33–35] we here designed a flow cytometry-based T_{CM} and T_{SCM} enrichment protocol in combination with the Prodigy process (Figure 3B). CD4 and CD8 T cells were retrieved after MACS bead separation on the Prodigy, and this population was antibody-stained for $CD95^+CD62L^+$ expression to enrich for T_{CM}

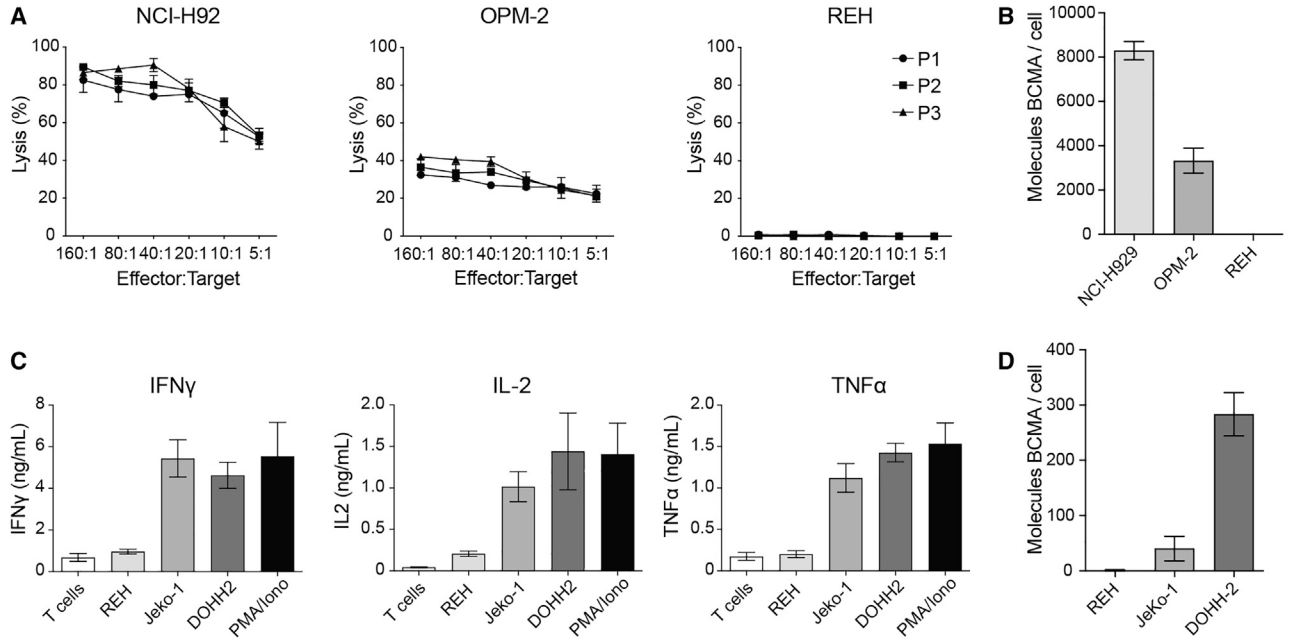

Figure 2. BCMA CAR T cells show antigen-specific effector functions toward BCMA-carrying tumor cell lines

(A) In a cytotoxicity assay, [^{51}Cr]-labeled cell lines with BCMA expression (NCI-H929 and OPM-2) and without BCMA expression (REH) (each 5 × 10^3) were co-cultured with BCMA CAR T cells at the indicated ratios for 4 h. Target cell lysis as [^{51}Cr] release was measured in duplicate in a γ-scintillation counter, and the results are displayed as mean ± SEM. (B) The expression of BCMA molecules on the surface of target cells was determined in a QuantiBRITE assay in three independent measurements and is displayed as mean ± SEM. (C) T cells (5 × 10^4) from run P1 (72.15% CAR$^+$), P2 (82.95% CAR$^+$), and P3 (80.10% CAR$^+$) were incubated in a 1:1 ratio with cell lines either expressing BCMA^{low} (JeKo-1, DOHH-2) or a BCMA-negative cell line (REH); n = 3 replicates per run. As a control, spontaneous cytokine release was determined by T cell culture only (min), and maximum release was stimulated with PMA/ionomycin (PMA/Iono); n = 1–3 replicates per run. Cell-free supernatants were harvested after 22 h to measure IFN-γ, IL-2, and TNF-α by ELISA. Bars represent mean ± SEM. (D) Expression of BCMA molecules on the surface of B-NHL target cells in this assay was determined using a QuantiBRITE assay in three independent measurements displaying mean ± SEM. Data are for n = 3 independent Prodigy runs.

and T_{SCM} subsets simultaneously. Next, cells were gently sorted by flow cytometry under aseptic conditions (Figure 3C). The T cell fraction obtained after MACS enrichment and the fluorescence-activated cell sorting (FACS)-sorted fraction were additionally stained (Figure S2B) to better discriminate T_{SCM} (CD95$^+$CD62L$^+$CD45RA$^+$CD45RO$^-$), T_{CM} (CD95$^+$CD62L$^+$CD45RA$^-$CD45RO$^+$), T effector (T_{EFF}; CD95$^+$CD62L$^-$CD45RA$^+$CD45RO$^-$), T_{EM} (CD95$^+$CD62L$^-$CD45RA$^-$CD45RO$^+$), and naive T (T_N; CD95$^-$CD62L$^+$CD45RA$^+$CD45RO$^-$) subpopulations. FACS resulted in a >5-fold enrichment of T_{CM} (56.55% ± 5.98% SEM) compared with the MACS fraction (10.64% ± 1.66% SEM). Similarly, we obtained a >3-fold enrichment of the T_{SCM} population compared with the MACS fraction (MACS, 3.54% ± 0.51% SEM; FACS, 11.89% ± 3.82% SEM) and a further enrichment at the end of the culture (HARV, 32.05% ± 7.01% SEM) (Figure 3C). To avoid extended FACS intervals (>2 h) that might impair the viability of the enriched T cell product, total T cell yield after cell sorting was intentionally limited to 15% of the numbers usually used in bulk runs (P1–P3) as input material for the Prodigy process (Table 2). T_{CM} and T_{SCM} subsets were not further separated but instead reapplied by sterile welding to the Prodigy tubing set. Combined T_{CM} and T_{SCM} were then cultured under the same stimulation conditions as for bulk runs, including IL-7 and IL-15 in the medium to better preserve a memory phenotype (Figure 3B).[36,37] However, the activity matrix was adapted according to the lower input of T cell numbers (Table 2).

Throughout the culture process, CD4$^+$ and CD8$^+$ T cell subsets were monitored for their memory phenotype (Figures 3D and S2B). Compared with the MACS products, FACS enriched CD4$^+$ T_{CM} cells >4-fold (64.44% ± 6.82% SEM) and >5-fold for CD4$^+$ T_{SCM} (12.18% ± 5.79% SEM), respectively. Strikingly, CD8$^+$ T_{CM} cells were enriched >9-fold (24.14% ± 2.77% SEM), and the CD8$^+$ T_{SCM} subset was increased by >10-fold (42.70% ± 3.94% SEM). During culturing, T_{SCM} increased to a frequency of 15.73% (±4.50% SEM) for CD4$^+$ and, most interestingly, to 63.33% (±6.69% SEM) for CD8$^+$ T cells in the HARV fraction (Figure 3D). The frequencies of T_{EM} (12.10% ± 0.08% SEM CD4$^+$, 1.57% ± 0.31% SEM CD8$^+$) and T_{EFF} (2.01% ± 0.44% SEM CD4$^+$, 7.12% ± 0.92% SEM CD8$^+$) subsets in the HARV fraction remained at minor levels. Most strikingly, when directly comparing the frequencies of T_{SCM} in either CD4$^+$ or CD8$^+$ T cell populations between bulk runs (P1–P3) and T_{CM}/T_{SCM} runs (P4–P6) in the final product (HARV), there was a significant increase in the proportions of T_{SCM} for the T_{CM}/T_{SCM} runs (Figure 3E).

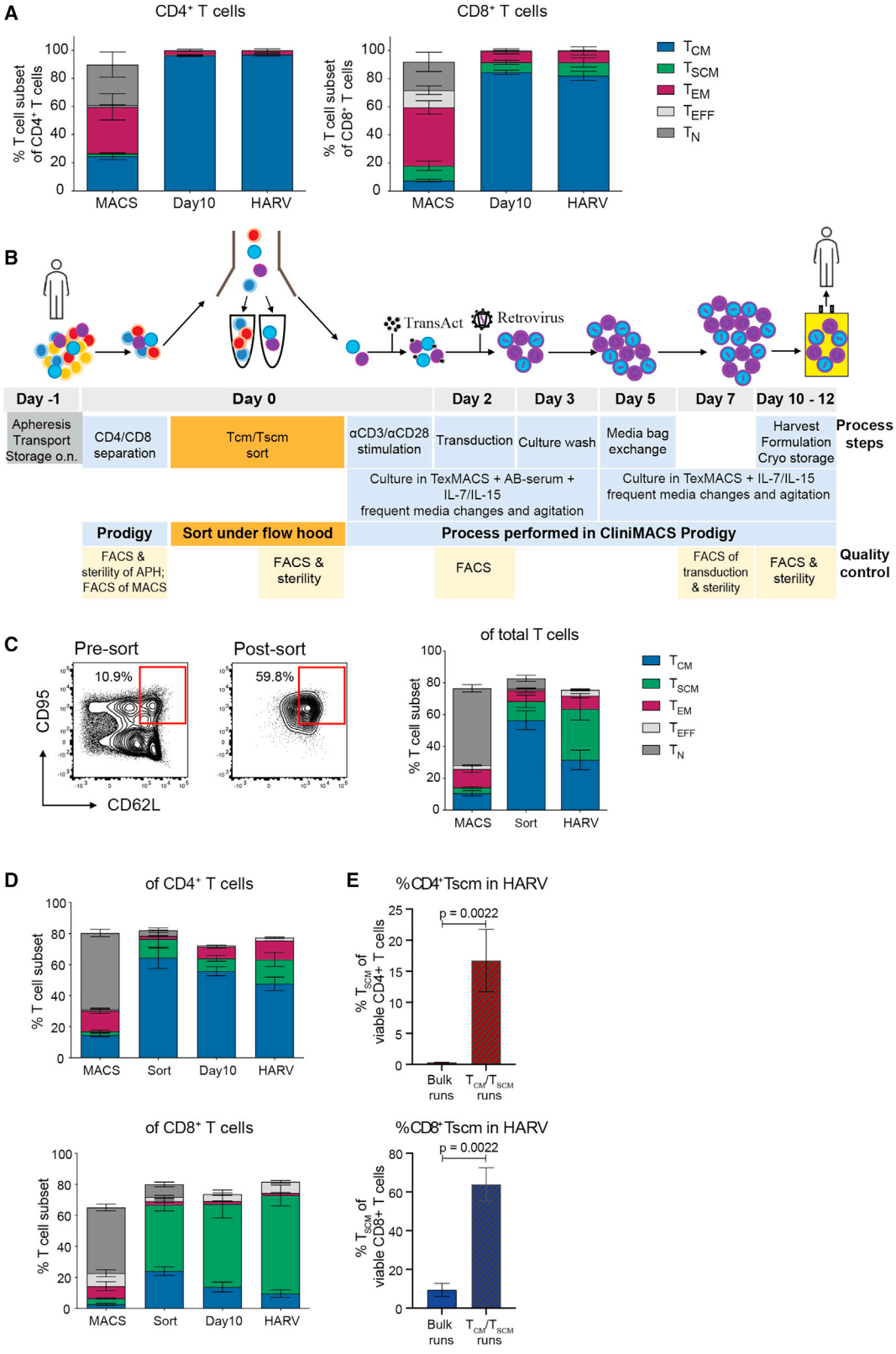

(legend on next page)

Some open process steps under a safety working bench were required to perform cell sorting by FACS, including disconnecting the reapplication bag containing MACS-separated cells, cell staining, and collection vessels, which might bear a risk for contamination. Because of careful aseptic handling, the microbiological controls of an in-process sample and the final product using aerobic and anaerobic culture bottles were negative.

Taken together, a combination of sterile cell sorting and an automated Prodigy bioreactor expansion allowed us to start with a small T cell input of a defined phenotype. This process resulted in engineered T cells with a preferential T_{CM} and T_{SCM} phenotype.

T_{CM} and T_{SCM} can be efficiently transduced with the BCMA CAR γ-retrovirus and expanded in an automated bioreactor process

In the T_{CM}/T_{SCM}-enriched fractions of runs P4, P5, and P6, also referred to as T_{CM}/T_{SCM} runs, the activation markers CD69 and CD25 were upregulated to a similar level at day 7 compared with the mixed T cell population in bulk runs (Figure 4A). It was not possible to determine the activation marker expression earlier, because of residual fluorescent sorting antibodies bound to the cells.

T_{CM}/T_{SCM} proliferated strongly during the cultivation course. At cell harvest, T_{CM}/T_{SCM} runs yielded between 1.49×10^9 and 2.28×10^9 T cells ($CD45^+CD3^+7\text{-}AAD^-$). This reflected an expansion rate of 166- to 706-fold, calculated from day 2, when initial cell numbers dropped because of activation induced cell death. T cell viability remained high at the end of each run ($7\text{-}AAD^-$) (Figure 4B; Table 2). Other non-T cell leukocyte subpopulations were efficiently reduced during CD4 and CD8 magnetic bead selection and decreased even stronger after FACS and throughout the bioreactor process (Figures 4C and S3A).

At cell harvest, a highly enriched cell product of 94.52% (±1.32% SEM) T cells and 4.13% (±1.21% SEM) NKT cells was recovered (Figure 4C). Residual $CD45^{int}CD34^+$ stem cells were essentially undetectable upon cell harvest (Figure 4D). During the culturing process, the $CD4^+$ T cell subset increased, and reciprocally, the $CD8^+$ fraction decreased (Figure 4E). Mixed T_{CM}/T_{SCM} fractions were retrovirally transduced with an MOI of 2 at 46 h after seeding. Transduction rates were between 41.1% and 62.6% and thus lower compared with the non-sorted T cell population (Figures 4F and 1G; Table 1). Indeed, we observed modestly lower transduction rates for T_{CM} and T_{SCM} compared with T_{EM} and T_{EFF} for all $CD3^+$ T cells and, even more strikingly, for $CD8^+$ T cell subsets (Figure S3B). The VCN per transduced T cell was between 2.4 and 3 retroviral copies per cell (Table 2). When gated on CAR^+ T cells first, a modest shift toward the $CD8^+$ subset occurred in the harvested product (Figure 4G). Together, regarding key parameters of the production process (Table 2), both groups, bulk runs and T_{CM}/T_{SCM} runs, had a similar amount of statistical variance within each group being compared.

To assess the functional competence of T_{CM}/T_{SCM}-derived BCMA CAR T cells, a co-culture assay with B-NHL cell lines was performed. T_{CM}/T_{SCM} BCMA CAR T cells produced high amounts of IFN-γ, IL-2, and TNF-α when challenged with $BCMA^{low}$-expressing DOHH-2 and JeKo-1 B-NHL cell lines. They produced only background levels when challenged with REH $BCMA^{neg}$ cells (Figure 4H). As previously observed for bulk runs, the release of effector cytokines was independent of BCMA surface expression levels, as DOHH-2 cells exhibited about 4 times more molecules compared with JeKo-1 cells (Figure 2D). To directly compare the cytolytic capacity of bulk run-derived $CD8^+$ BCMA CAR T cells with those from T_{CM}/T_{SCM} runs, $CD8^+$ enriched BCMA CAR T cells were co-cultured with $BCMA^{high}$ (MM.$1S^{BCMA\text{-}high}$.eGFP), $BCMA^{low}$ (MM1.$S^{BCMA\text{-}low}$.eGFP, JeKo-1.eGFP, DOHH-2.eGFP), and $BCMA^-$ (REH.eGFP) target cells (Figure 5A). For the MM.$1S^{BCMA\text{-}high}$ target cells, in this flow cytometry-based assay the efficiency of killing was nearly 100% for all effector CAR T cell preparations, even at very low effector to target ratios (Figure 5B). In contrast, for the $BCMA^{low}$-expressing cell lines, a trend toward improved cytolytic functionality for T_{CM}- and T_{SCM}-derived effectors was observed

Figure 3. T_{CM}/T_{SCM} T cells can be enriched using FACS and are suitable for BCMA CAR T cell production in the CliniMACS Prodigy

(A) $CD4^+$ T cells (left) and $CD8^+$ T cells (right) from bulk runs P1–P3 were analyzed for T cell subset composition at the indicated process steps. The gating for each subpopulation was done as follows: T central memory (T_{CM}), $CD95^+CD62L^+CD45RO^+$; T stem cell memory (T_{SCM}), $CD95^+CD62L^+CD45RO^-$; T effector memory (T_{EM}), $CD95^+CD62L^-CD45RO^+$; T effector (T_{EFF}), $CD95^+CD62L^-CD45RO^-$; T naive (T_N), $CD95^-CD62L^+CD45RO^-$. Representative gatings are shown in Figure S2A. (B) Schematic representation of the BCMA CAR T cell process with an integrated aseptic sorting of T_{CM} and T_{SCM}. CD4/CD8 T cells were retrieved from the apheresis material using magnetic cell sorting on the CliniMACS Prodigy platform (day 0). MACS-enriched T cells were stained with anti-CD95 and anti-CD62L antibodies, followed by sorting for $CD95^+CD62L^+$ T_{CM}/T_{SCM} subsets on a droplet sorter located under a laminar flow hood (orange boxes). Sorted T_{CM}/T_{SCM} cells were then reinserted into the tubing set on the bioreactor and stimulated with α-CD3/α-CD28 coated TransAct beads. Media were used as in Figure 1A. Retroviral transduction, serum-free media exchange, and final product harvest was done as indicated. T cells were formulated and cryopreserved between days 11 and 12 of culture. Culture conditions, absence of bacteria and fungi, and cell phenotype were analyzed during the whole process (yellow boxes). (C) CD4/CD8 MACS-separated cells were stained and FACS-sorted for a T_{CM}/T_{SCM} ($CD95^+CD62L^+$) enriched population. Cells in the sort gate were analyzed pre-sort (left FACS plot) (MACS step) and post-sort (FACS step, right FACS plot). Numbers on the gates indicate percentages of cells defined as $CD95^+CD62L^+$ T_{CM}/T_{SCM}. On the right, bar graph shows the quantitative analysis of subset composition in the MACS, in the FACS-sorted fraction, and the final product (HARV). Subpopulations were gated as follows: T_{CM}, $CD95^+CD62L^+CD45RO^+CD45RA^-$; T_{SCM}, $CD95^+CD62L^+CD45RO^-CD45RA^+$; T_{EM}, $CD95^+CD62L^-CD45RO^+CD45RA^-$; T_{EFF}, $CD95^+CD62L^-CD45RO^-CD45RA^+$; T_N, $CD95^-CD62L^+CD45RO^-CD45RA^+$. (D) $CD4^+$ T cells (top) and $CD8^+$ T cells (bottom) were analyzed for T cell subsets at defined intervals (MACS, sort, day 10, HARV). Subpopulations were gated as in (C). Example dot plots are shown in Figure S2B. (E) Comparison of the frequency of T_{SCM} in $CD4^+$ T cells (upper panel) and $CD8^+$ T cells (lower panel) in the harvest (HARV) gated according to gating scheme in Figure S2A. Statistical analysis was done using a Mann-Whitney U test. All samples were run in technical duplicate, and results are displayed as mean ± SEM (A and C–E). Figures show data for n = 3 independent Prodigy runs for each condition: bulk runs and T_{CM}/T_{SCM} runs.

Table 2. Quantification of process efficiency using enriched T_{CM}/T_{SCM} cells as starting material in P4–P6

Run	Starting Cell No.	Process Duration	CD4/CD8 Ratio in HARV	Expansion Rate[a]	T Cell No. in HARV	Transduction Rate of $CD45^+CD3^+$ in HARV	CAR T Cell No. in HARV	VCN
P4	0.12×10^8	11 days	73.2%/26.0%	166×	1.49×10^9	62.6%	0.93×10^9	3.0
P5	0.15×10^8	12 days	85.9%/9.6%	706×	2.20×10^9	41.1%	0.90×10^9	2.4
P6	0.14×10^8	12 days	85.9%/9.6%	305×	2.28×10^9	58.6%	1.34×10^9	ND

n.d., not done.
[a]The expansion rate was calculated from day 2 on.

(Figures 5C–5E). $BCMA^-$ REH cells were not killed specifically (Figure 5F).

Repetitive antigen stimulation *in vitro* reveals comparable effector functions and proliferative capacity of non-sorted and T_{CM}/T_{SCM}-derived BCMA CAR T cells

To mimic chronic antigen stimulation *in vitro*, a repetitive antigen stimulation assay was performed.[28,38] BCMA CAR T cells were recursively co-cultured with $BCMA^{high}$ MM1.S.eGFP cells, which were replenished every 3 days. As parameters of T cell exhaustion and functionality, tumor cell killing, CAR T cell proliferation, IFN-γ secretion, and surface-deposited exhaustion markers were determined. Both types of BCMA CAR T cell preparations, bulk derived or T_{CM}/T_{SCM} derived, showed efficient and constant killing over five rounds of co-culture (Figure 6A). Additionally, the production of IFN-γ declined for both production conditions; unexpectedly, this decrease was even stronger for the T_{CM}/T_{SCM}-derived culture supernatants (Figure 6B).

The proliferation capacity was modestly reduced for the T_{CM}/T_{SCM} runs from the second round of re-stimulation (Figure 6C), and repetitive antigen stimulation induced an enrichment of the CAR^+ T cell population to almost 100% (Figure 6D). The CD4/CD8 ratios shifted toward a higher $CD8^+$ fraction (Figure 6E). Interestingly, in the T_{CM}/T_{SCM} runs (CD4/CD8, 85%:15%), which initially contained less $CD8^+$ T cells than the bulk runs (CD4/CD8, 70%:30%), the $CD8^+$ fraction was enriched much stronger than in the non-sorted T cell population. This may indicate a stronger proliferative potential of $CD8^+$ T_{CM}/T_{SCM} cells compared with $CD4^+$ T cells. The kinetics of exhaustion marker expression for TIM-3, PD-1 and LAG-3 behaved similarly for both sets of conditions, except for LAG-3 in the $CD8^+$ BCMA CAR T cell subset (Figure 6F).

To adjust the proportions of $CD8^+$ CAR^+ T cell subsets (Figures 1G and 1H vs. Figures 4F and 4G), we repeated the *in vitro* repetitive antigen stimulation assay with separated $CD8^+$ BCMA CAR T cells. $CD8^+$ CAR T cells from both preparations killed $BCMA^{high}$ MM1.S.eGFP very efficiently over seven rounds of co-culture (Figure S4A). As observed before (Figure 6), IFN-γ declined over time, with the decrease being even stronger for the T_{CM}/T_{SCM}-derived culture supernatants (Figure S4B). $CD8^+$ BCMA CAR T cells from bulk runs initially proliferated till passage 4 (day 12) but thereafter declined to a rate of only 1.5-fold. In contrast, CAR T cells from T_{CM}/T_{SCM} runs did not expand substantially over the stimulation period of 21 days (Figure S4C). The enrichment of the CAR^+ $CD8^+$ T cell population was much weaker compared with mixed $CD4^+$ and $CD8^+$ CAR^+ T cells (Figure S4D). This indicated that the proliferation rate and CAR T cell enrichment were strongly dependent on the presence of $CD4^+$ T cells in this assay.[39]

Phenotypic T_{SCM} markers such as CCR7 and CD45RA were strongly downregulated during recursive antigen challenge in both sets of CAR T cell preparations, whereas the T_{SCM} and T memory and activation marker CD95 was upregulated and remained at a plateau. CD62L was stronger expressed on bulk BCMA CAR T cells compared with the T_{CM}/T_{SCM} run BCMA CAR T cell preparations. In conjunction with an increasing CD45RO expression, this may indicate the induction of a growing number of antigen-experienced memory-type CAR T cells (Figure 6G).

In addition to phenotypic marker characterization, we examined the transcriptional profile of a limited set of genes indicative of T_{EFF}, T_{CM}, or T_{SCM} differentiation (Figure 6H). The T_{SCM} and T_{CM} regulating transcription factor TCF7, which maintains stemness properties, showed essentially no change in expression compared with the MACS cell population; the latter predominantly consisted of naive T cells and was set here as reference gene expression. Constitutive activation of the TCF7-Wnt/β-catenin pathway *in vivo* favors the generation of memory $CD8^+$ T cells.[40] Transcription factors that are also shared between T_{SCM} and T_{CM}, such as ID3 and LEF1, were largely indistinguishable between both CAR T cell production conditions. $ID3^{high}$ is abundantly expressed in long-lived memory cell precursors. ID3 itself is repressed by PRDM1 (BLIMP1), a strong promoter of terminal effector cell differentiation. Similar to TCF7, LEF1 is a downstream effector of the WNT signaling pathway and thus cooperatively supports the development of memory precursor and memory T cells.[41] BCL2, a leading factor conferring anti-apoptotic functions in memory T cell development, was also not altered. The transcription factors PRDM1 (BLIMP1) and TBX21 (T-bet) were upregulated for all Prodigy runs, but TBX21 was 2.3-fold higher in bulk runs (5.17 for P1/P2 vs. 2.18 for P4/P5), indicating a predominance of terminal effector T cells. IFNG as a typical effector T cell-associated gene function was higher upregulated for runs P1 and P2, suggesting that more terminal effector-like CAR T cells existed. On the other hand, much lower expression for IFNG in T_{CM}/T_{SCM} runs would be consistent with the stronger presence of less differentiated T_N and potentially T_{SCM} cells as well (Figure 6H).

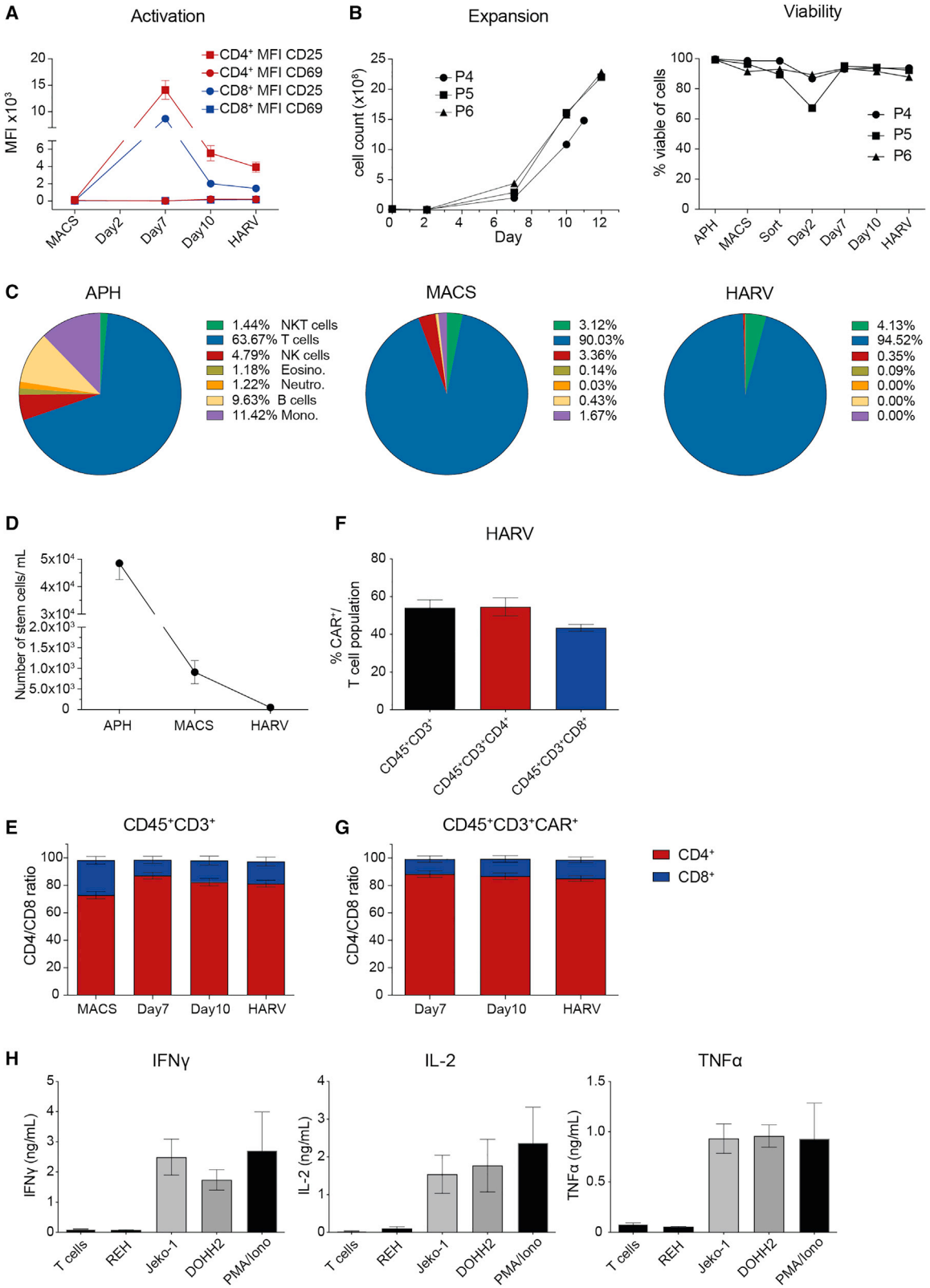

(legend on next page)

Taken together, BCMA CAR T cells from bulk runs and those derived from T_{CM}/T_{SCM} enrichment showed similar cytotoxic capacity. Lower IFN-γ secretion in the T_{CM}/T_{SCM}-enriched population was consistent with the gene expression profile observed in BCMA CAR T cell products from runs P4 and P5.

DISCUSSION

In this study we show that the generation of functionally active BCMA CAR T cells in an automated GMP-compliant system can be adapted to the needs of a preferential T_{CM} and T_{SCM} CAR T cell production. We implemented a strategy for the production of clinically relevant amounts of γ-retrovirally transduced BCMA CAR T cells, starting with a T cell population that contained heterogeneous maturation stages. The automated CliniMACS Prodigy process yielded high transduction rates, stable CD4/CD8 ratios, elimination of hematopoietic stem cells, strong proliferative and cytotoxic capacity, and preferential T_{CM} differentiation. The γ-retroviral system allowed high transduction rates at low VCN integrations.

Although clinical advantages of CAR-engineered T_{CM} cells in lymphoid malignancies have been proposed, clinical exploitation of potentially superior T_{SCM} differentiated CAR T cells is hampered by the relative paucity in circulation and lack of clinical grade protocols for T_{SCM} isolation.[9,16,42–44] Here, we established a protocol in which the automated GMP-compliant bioreactor protocol was combined with a flow cytometry-based enrichment of T_{CM} and T_{SCM} T cells as input material. As a drawback of this procedure, to our knowledge, GMP-compliant FACS devices have currently no regulatory European Medicines Agency (EMA) approval. In contrast, magnetic bead sorting for the enrichment of T cells with T_{CM} or T_{SCM} phenotypes requires several sequential manual open steps under clean room conditions. In general, these steps are not only lengthy but are of low efficiency, are error prone, and bear higher risks for contamination. A flaw of our FACS protocol is the use of leukapheresis material from healthy donors, which might not properly reflect the duration of the sorting process for T cells derived from leukopenic tumor patients.

In our process, starting with only an eighth of the Prodigy standard input material, the T_{CM}- and T_{SCM}-enriched fraction expanded to clinically relevant numbers of BCMA CAR T cells, featuring comparable cytotoxic effector functions, cytokine production, and low expression of exhaustion markers. Of note, in a small-scale experiment, the use of similar starting cell numbers of either bulk or T_{CM}/T_{SCM} input material from the same donor did not result in statistically different T cell expansion for T_{CM}/T_{SCM} input material, either at low (1.5×10^5) or at high (1×10^6) T cell input cell numbers (data not shown). Low input of T cells may well reflect the situation of critically ill patients that have usually received multiple lines of myelosuppressive chemotherapy for the treatment of multiple myeloma. Notably, in the T cell product, the proportion of T_{SCM} in the $CD8^+$ subset was much higher than in the $CD4^+$ population. Compared with non-sorted T cells in bulk runs, a larger fraction of T_{SCM} CAR T cells was generated in the 11- to 12-day production process. Interestingly, in the repetitive antigen stimulation assay, isolated $CD8^+$ BCMA CAR T cells, derived from either T_{CM} or T_{SCM} precursors, performed weaker than the non-sorted BCMA CAR T cells, visible as lower proliferation rate. This suggests that $CD4^+$ T cells have a crucial role in the maintenance of $CD8^+$ T cell memory and expansion, whereas a split production might be disadvantageous in this regard.[39] Furthermore, *in vitro* repetitive antigen stimulation studies cannot fully recapitulate persistence *in vivo*. Others have shown that engraftment and expansion of engineered T cells positively correlated with the infusion of early memory T cells[7,10] and that fully developed effector populations showed impaired *in vivo* function after transfer.[45] Accordingly, the true functional and proliferative potential of $T_{SCM\ and}$ T_{CM} CAR T cell populations are likely to be much better assessed in clinical studies. An unexpected challenge in our aim to generate a preferential T_{CM}- and T_{SCM}-skewed BCMA CAR T cell product was the phenotypic definition of T_{SCM} cells. In the pioneering work by Gattinoni et al.,[46] T_{SCM} were identified in peripheral human blood and characterized under homeostatic conditions. The antigen-specific memory was defined by the responsiveness of the TCRs toward previously encountered viral and self-tumor antigens. These cells were found within a $CD45RO^-CCR7^+CD45RA^+CD62L^+CD27^+CD28^+$ and IL-$7Ra^+$ T cell compartment. They were discriminable from T_N by the strong co-expression of CD95, CD122, CXCR3, and other attributes. In addition, the homeostatic chemokine receptor CCR7 was also used as a characteristic T_{SCM} maturation marker. When stimulated with IL-15 alone, T_{SCM} cells maintained $CD45RA^+CCR7^+CD62L^+$ $CD45RO^-$ expression.[46] In contrast, a strong α-CD3/α-CD28 stimulation gradually upregulated CD45RO, characteristic of activated memory T cells, while downregulating CD62L and CCR7. These changes were interpreted as capacity of multipotent T_{SCM} to give rise to diverse progeny. Similar observations were made in our study

Figure 4. T_{CM} and T_{SCM} are efficiently transduced with the BCMA CAR encoding γ-retrovirus in the Prodigy process

(A) T cell activation determined by staining with anti-CD25 and anti-CD69 antibodies on $CD4^+$ and $CD8^+$ viable 7-$AAD^-CD45^+CD3^+$ T cells. Values represent mean fluorescence intensity (MFI), minus an isotype control. (B) Total number of $CD3^+$ T cells (left) and their viability (7-AAD^-) (right) was measured. (C) Cellular composition at different bioreactor process steps. Leukocyte subsets were defined as in Figure 1D. The pie charts represent the mean of n = 3 Prodigy runs. (D) Numbers of $CD45^{int}CD34^+$7-AAD^- stem cells in the apheresis material (APH), in the MACS fraction, and in the final product (HARV) were determined as in Figure 1E. (E) Ratios of $CD4^+$ and $CD8^+$ 7-$AAD^-CD45^+CD3^+$ T cells in the culture over the whole process. (F) Frequency of CAR^+ T cells among all T cells (7-$AAD^-CD45^+CD3^+$) and on the T cell subpopulations (7-$AAD^-CD45^+CD3^+CD4^+$ and 7-$AAD^-CD45^+CD3^+CD8^+$) was determined for the final product (HARV). (G) CAR T cell transduction rate among $CD4^+$ and $CD8^+$ T cells. Samples were run in duplicates, and results are displayed as mean only (C), or mean ± SEM (A, B, and D–G). (H) T cells (5×10^4) from P4 (62.6% CAR^+), P5 (41.1% CAR^+), and P6 (58.6% CAR^+) were co-cultured in a 1:1 ratio with cell lines expressing either $BCMA^{low}$ (JeKo-1 and DOHH-2) or $BCMA^-$ (REH); n = 3 replicates per run. Maximum cytokine release was induced by T cell stimulation with PMA/ionomycin (PMA/Iono); min is T cells only. Cell-free supernatants were harvested after 22 h to measure IFN-γ, IL-2, and TNF-α by ELISA; bars represent mean ± SEM. Data are for n = 3 independent Prodigy runs.

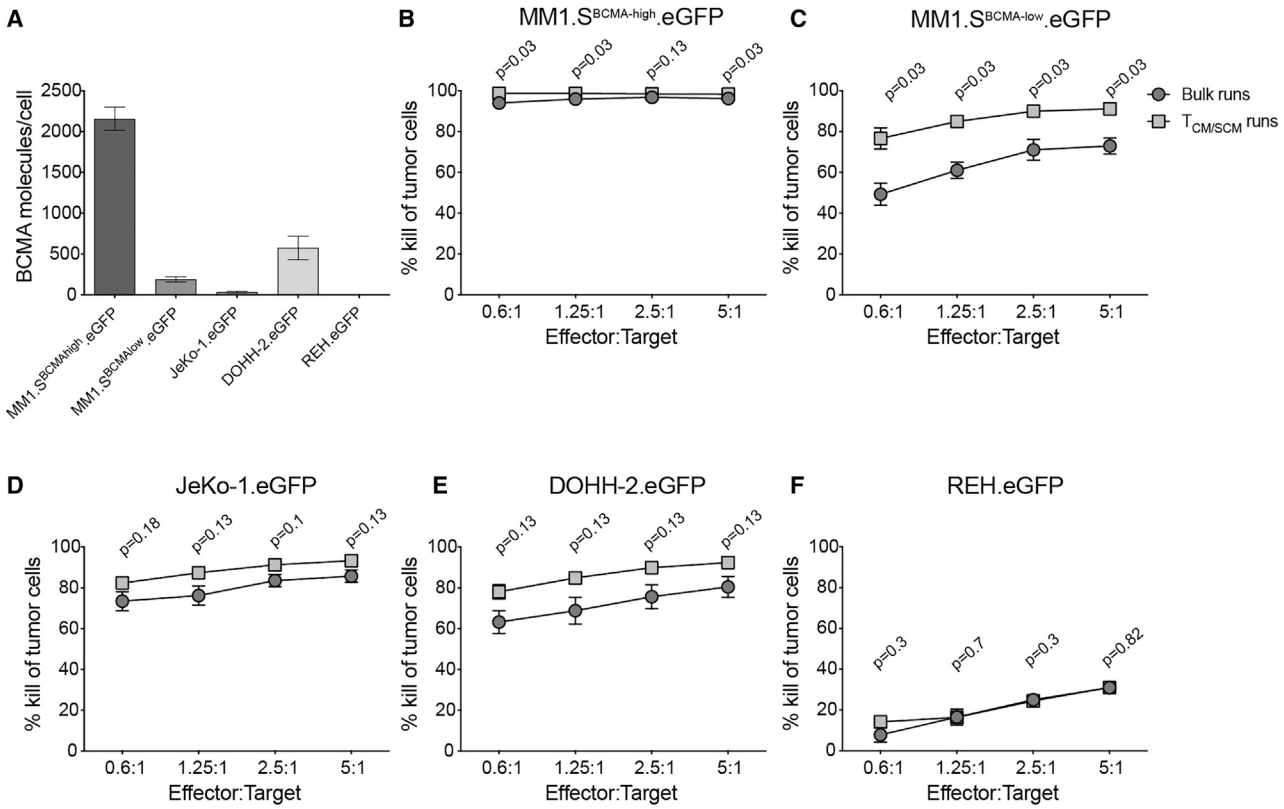

Figure 5. Similar cytolytic activity of bulk and T_{CM}/T_{SCM}-derived BCMA CAR T cells

(A) BCMA surface expression of the target tumor cell lines was determined in a QuantiBRITE assay in two or three independent measurements. Cell lines with (B) $BCMA^{high}$ expression (MM.1S$^{BCMA\text{-}high}$.eGFP), (C–E) $BCMA^{low}$ expression (MM1.S$^{BCMA\text{-}low}$.eGFP, JeKo-1.eGFP and DOHH-2.eGFP), and (F) without BCMA expression (REH.eGFP) (each 5×10^4) were co-cultured with CAR T cells from bulk runs P1–P3 and T_{CM}/T_{SCM} runs P4–P6 at the indicated effector to target ratios for 24 h. Target cell lysis was determined by tumor cell counting (7-AAD$^-$CD3$^-$GFP$^+$) on a MACSQuant analyzer. The numbers of remaining tumor cells in the culture are normalized to tumor cells grown without the addition of T cells. The results are displayed as mean ± SEM. Statistical analysis was performed using a Mann-Whitney U test for each E/T ratio. Data are for n = 3 independent Prodigy runs for each condition.

where input T_{SCM} were engineered to express a BCMA CAR. In this process, a brief proliferation stimulus together with the introduction of a retrovirus may affect differentiation processes in CAR T cells and thus, prohibit a clear definition of T_{SCM} phenotypes. As a result of the complex T cell engineering during the BCMA CAR T bioreactor process, CCR7 declined strongly. Thus, for the T_{CM}/T_{SCM} isolation process, we here relied on the differentiation markers CD95 and CD62L, while the in-process quality control involved CD45RA, CD95, CD62L, and CD45RO. To further substantiate lineage differentiation, we selected a few genes indicative of T_{SCM}, T_{CM}, and T_{EFF}. Because of a largely overlapping gene expression pattern of memory defining TCF7, ID3, LEF1, and BCL2[47] gene expression in T_{SCM} and T_{CM}, a difference between the bulk-derived and T_{CM}/T_{SCM}-derived CAR T cell products was not obtained. Notably, bulk runs already yielded up to 90% of all T cells with a T_{CM} differentiation, the size of which was similar to the combined T_{CM} and T_{SCM} compartment in T_{CM}/T_{SCM} runs. On the other hand, strong upregulation of the T-box transcription factor Eomesodermin (EOMES) in CAR T cells in T_{CM}/T_{SCM} run P4 and low expression of its opposing partner TBX21 responsible for terminal effector T cell differentiation would be consistent with a preferential memory differentiation in the CAR T cell product. The increased expression of TBX21 in the BCMA CAR T cell product indicated a skewing in differentiation toward the Th1 ($CD4^+$) and Tc1 ($CD8^+$) lineages, which corresponded to an increased production of IFN-γ upon stimulation with $BCMA^+$ MM.1S cells.[48,49] High expression of TBX21 in T cells lacking concomitant high expression of EOMES also indicated a differentiation toward T_{EM}.[21,50,51] In keeping with a smaller proportion of acute effector BCMA CAR T cells from T_{CM}/T_{SCM} runs P4 and P5, much lower gene expression for IFNG indicated the stronger presence of less differentiated T_N and potentially T_{SCM} cells as well, because the IFNG genetic locus is less accessible in naive T cells.[52,53] We conclude that the cells generated in T_{CM}/T_{SCM} runs reflect a preferential T_{SCM}/T_{CM} maturation stage as signified by their surface marker expression and their mRNA profile. However, further *in vivo* studies ideally involving clinical trials are needed to confirm the phenotypic and functional relevance of this phenotype.

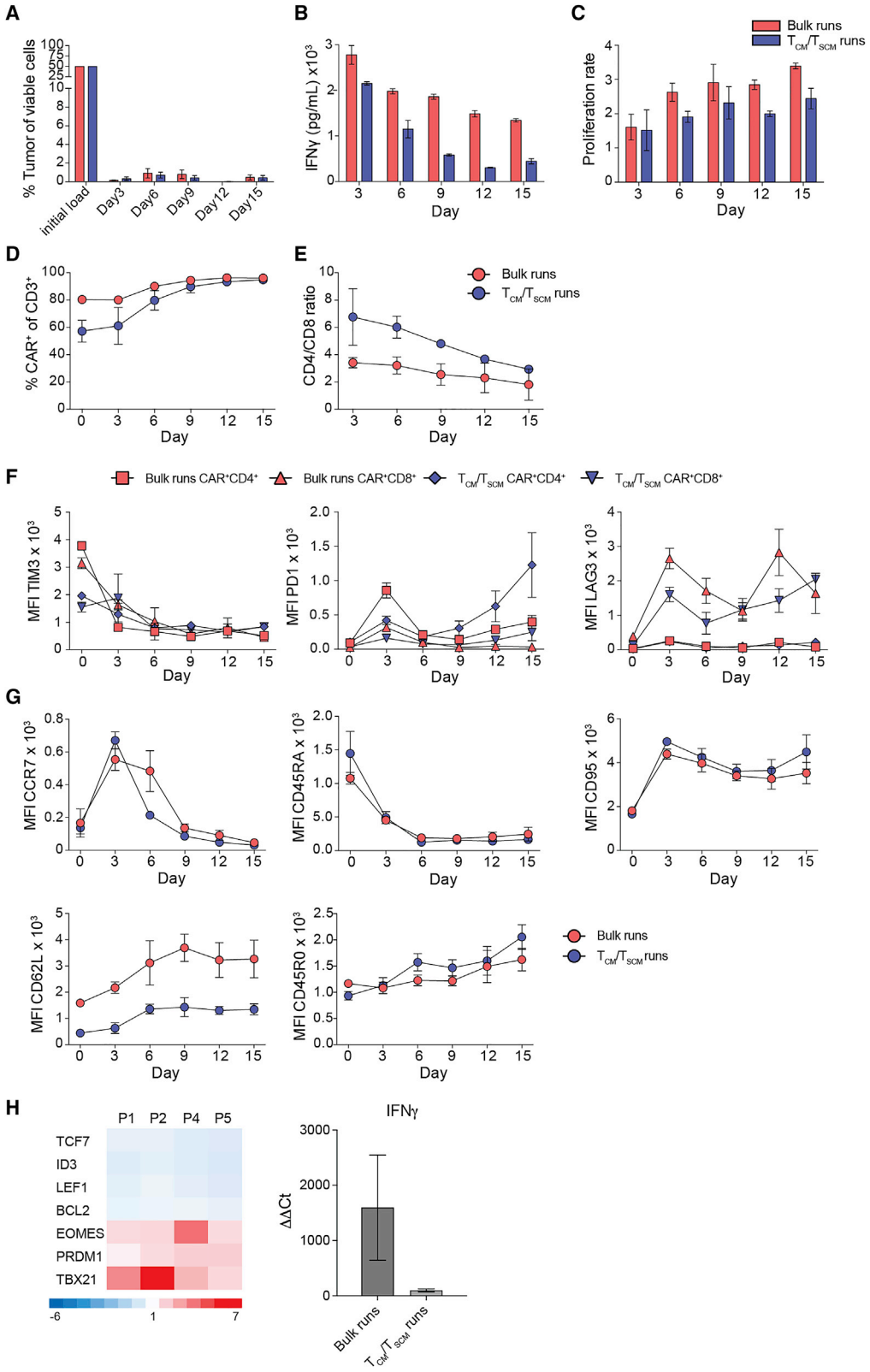

(legend on next page)

In a previous report,[9] CAR-modified $CD8^+$ memory stem cells were generated by bead enrichment of T_N cells, followed by cell activation and culturing in the presence of IL-7, IL-21, and the GSK-3β inhibitor TWS119. By activation of the Wnt/β-catenin signaling pathway, T_N preferentially differentiate into the T_{SCM} lineage. In contrast to our results, significant differences in the release of IFN-γ between a standard CD19 CAR T cell protocol and the T_{SCM}-derived $CD8^+$ CAR T cell population were not detected. We conclude that substantial differences in the generation of T_{CM} and T_{SCM} CAR T cell products might account for these differences. Whereas we started with T_{CM} and T_{SCM} cells that were supported by IL-7 and IL-15 in a clinical-scale Prodigy protocol, Sabatino et al.[9] used T_N as input for the generation of T_{SCM}-derived CD19 CAR T cells. In this process, Wnt/β-catenin activation in conjunction with very low T cell expansion rates are likely to induce different maturation pathways and other functional outcomes. Priming naive $CD8^+$ T cells in the presence of IL-7 and IL-15 has been proposed to be an effective method to generate T_{SCM} from a T_N input population.[37] However, gene expression profiles of T_N-derived T_{SCM} generated in an IL-7/IL-21/TWS119 cell culture protocol, but not from an IL-7/IL-15 cell culture, have a higher similarity to naturally occurring T_{SCM}. We conclude that different input differentiation stages, variable cytokine and pharmacological inhibitor cocktails, cell culture duration, and scale might critically affect phenotypic and functional properties of the harvested CAR T cell product. Moreover, the modular design of the CAR potentially influences T cell differentiation by causing various levels of tonic signaling.

Finally, in order to aim for a fully GMP-compliant FACS protocol that can provide sufficient T_{SCM} cells for a subsequent large-scale Prodigy process, new sorting devices in conjunction with Conformité Européenne (CE)-certified antibodies for fluorescent detection and cell labeling are currently under development. This technical solution may accelerate a broader and standardized application of T_{SCM} as starting population for CAR T cells with improved *in vivo* expansion, longevity and extended tumor control.

For our CAR construct we used human CD28 as a costimulatory domain, which has advantages regarding rapid tumor elimination[54] and resistance upon immunosuppressive TGF-β signaling.[55] Alternatively, data suggest that CAR T cells equipped with a human 4-1BB costimulatory domain exhibit longer *in vivo* persistence, which is likely caused by a different metabolic programming.[56] In the absence of side-by-side comparisons, it is unclear whether CAR T cells equipped with a 4-1BB costimulatory domain in context of a preferential T_{SCM} phenotype will be of advantage for CAR T cell persistence, proliferation, and prolonged tumor control. We infer, that the use of selected T cell starting populations, either with preferential effector functions or preferential stem-like T cells, must be adapted to the needs of specific tumor entities. Although preclinical assessments on the role of costimulatory domains, or CAR T cell differentiation states can be indicative of anti-tumor efficacy and safety, a validation of these aspects, or even proof of superiority over other constructs applied to a specific tumor entity require comparative approaches.[57] These must be conducted according to phase 3 clinical trial designs. An important step in that regard will be the harmonization of the T cell input material for which we propose to use T_{SCM}.

MATERIAL AND METHODS

Human PBMCs

Leukapheresis from healthy volunteers was performed at the Charité Stem Cell Facility (SCF Charité, Berlin, Germany). Written informed consent was given by all apheresis donors. The study was performed according to the Declaration of Helsinki and in accordance with local ethical guidelines. An ethics vote was conducted at Charité-University Medicine Berlin. Fresh apheresis material was stored overnight at 4°C and further processed at room temperature the next day.

Retroviral vector

A BCMA CAR γ-retroviral vector was generated as described.[28] The vector encodes a second-generation CAR with a fully humanized single-chain variable fragment (scFv) directed toward BCMA, a CD28 costimulatory domain, and a CD3ζ activation domain, which endows T cells with a high-affinity CAR directed against BCMA. This MP71 vector-based construct was subcloned into a γ-retroviral self-inactivating (SIN) vector pES.12-6 vector (BIONTECH Innovative Manufacturing Services, Idar-Oberstein, Germany). A producer cell clone, a primary seed bank and a master cell bank were generated using the 293VecGaLV producer cell line (BioVec, Québec, Canada). In short, the CAR construct was cloned into the SIN γ-retroviral vector backbone and by targeted integration, a producer cell clone was generated by *Flp*-recombinase-mediated cassette exchange (*Flp*-

Figure 6. Sustained antigen exposure *in vitro* reveals similar effector function of bulk- and T_{CM}/T_{SCM}-derived BCMA CAR T cells.

BCMA CAR T cells from bulk runs P1/P2 and T_{CM}/T_{SCM} runs P4/P5 were co-cultured in a 1:1 ratio with MM1.$S^{BCMA\text{-}high}$.eGFP target cells. After 72 h, CAR T cells were retrieved and co-cultured with fresh MM1.$S^{BCMA\text{-}high}$.eGFP target cells, for a total of 5 transfer rounds. Data are presented as mean ± SEM. (A) Quantification of residual viable MM1.$S^{BCMA\text{-}high}$.eGFP target cells (7-$AAD^-CD3^-GFP^+$) by flow cytometry analysis after each round of co-culture. (B) Cell-free supernatants were harvested after each round and analyzed using ELISA for IFN-γ release (n = 4 replicates per run). (C) After each round, viable 7-AAD^-CD3^+ T cells were counted, and the proliferation rate was calculated as the ratio of input T cells versus T cell numbers after 72 h. (D) Frequency of transduced CAR^+ T cells was measured among viable $CD3^+$ T cells. (E) Ratio of $CD4^+$ to $CD8^+$ T cells among all $CD3^+$ T cells was measured after each round. (F) Viable 7-AAD^-CAR^+ $CD4^+$ or $CD8^+$ T cells were analyzed for their expression of the exhaustion markers TIM-3, PD-1, and LAG-3. Data represent the MFI subtracted by the values of the isotype control. (G) 7-$AAD^-CD3^+CAR^+$ T cells were analyzed for their expression of T cell memory markers CCR7, CD45RA, CD95, CD62L, and CD45RO. Data represent MFI subtracted by the values of the isotype control and are displayed as mean ± SEM. (H) The mRNA expression of the depicted genes was determined using qRT-PCR and analyzed with the ΔΔCt method by first calculating each sample relative to the expression of the house keeper gene B2M. Values are then depicted as gene regulation in the harvested product relative (x-fold) to the corresponding MACS sample. Expression changes ranging from −6 to 7 are presented in the heatmap (left), and expression changes of IFNG is depicted as bar graph. A color scale is depicted on the bottom. (A), (C), (D), and (G) represent data from two independent experiments. (B), (F), and (H) represent data from one experiment.

RMCE) with the introduced sequence immobilized (BIONTECH Innovative Manufacturing Services). Finally, a Cre-mediated cleanup step was used to establish a safe retroviral producer cell line. The CAR is under the control of a hEF1α promoter. Clinical grade viral supernatant was produced and titrated on Jurkat cells (T-ALL). Retrovirus was stored at −80°C.[58,59] The viral supernatant was tested for replication-competent retrovirus (RCR) by direct inoculation and cocultivation method (293 enrichment cells and PG4 S+L detection cells; assays performed by BIONTECH and BioReliance). No RCR was detected in the viral supernatant.

Automated CAR T cell production

Automated CAR T cell production was performed on the CliniMACS Prodigy (Miltenyi Biotec, Bergisch-Gladbach, Germany) device using the GMP-grade TS520 tubing set for T cell transduction and culture. The standard TCT protocol provided by the manufacturer was modified according to a retrovirus-optimized design. All runs were performed using software version 1.3. Initially, the apheresis material was introduced into the device, washed with GMP-grade PBS/EDTA (Miltenyi Biotec) supplemented with 0.5% HSA (CSL Behring, Marburg, Germany), and magnetically separated using GMP-grade CD4 and CD8 Reagent (both from Miltenyi Biotec). The enriched $CD4^+/CD8^+$ cells were seeded at a concentration of 1×10^8 T cells in medium 1, consisting of GMP-grade TexMACS medium (Miltenyi Biotec), 1% AB serum (Sigma-Aldrich/Merck, Darmstadt, Germany; or ZKT, Tübingen, Germany), 12.5 ng/mL IL-7 and 12.5 ng/mL IL-15 (premium grade; Miltenyi Biotec). T cells were activated immediately with GMP-grade TransAct (α-CD3/α-CD28 coated beads) (Miltenyi Biotec). T cell transduction was performed 46 h after seeding with an MOI of 2 and the addition of Vectofusin-1 in serum-free medium 2, consisting of GMP-grade TexMACS medium with 12.5 ng/mL IL-7 and 12.5 ng/mL IL-15. Cells were spun at 400 × *g* for 2 h at 32°C. After 24 h, a culture wash was performed to remove the remaining virus and activation beads. From day 5 on, medium 1 was gradually exchanged with medium 2 to reduce the amount of residual AB serum till the end of culture. Transduced CAR T cells were cultured following a regime of frequent medium changes and agitation till final formulation in NaCl (B. Braun, Melsungen, Germany) supplemented with 0.5% HSA between day 10 and day 12 of culture. After the final formulation T cells were prepared for cryoconservation in a 1:1 ratio with NaCl supplemented with 5% HSA and 20% DMSO (CryoSure, WAK-Chemie, Steinbach, Germany). Cells were stored for further analysis in liquid nitrogen. For runs involving FACS steps, medium 1 containing additionally 1% penicillin/streptomycin (PAN-Biotech, Aidenbach, Germany; penicillin 10,000 U/mL and streptomycin 10 mg/mL) and 1% gentamycin (10 mg/mL; Biochrom, Berlin, Germany), and medium 2 containing additionally 1% penicillin/streptomycin were used. Supernatant from samplings at day 10 did not contain infectious residual virus. This was shown by a CAR-specific FACS stain (anti-IgG-PE) 3 days after spinoculation (800 × *g*, 90 min, 32°C) of highly susceptible Jurkat T-ALL cells with day 10 sampling supernatant (data not shown).

Flow cytometry-based sorting of T_{CM} and T_{SCM} for automated CAR T cell production

For sterile sorting of T_{CM} and T_{SCM} cells from CD4/CD8 MACS separated cells, the $CD4^+$ and $CD8^+$ T cell-containing MACS fraction was recovered from the reapplication bag on the CliniMACS Prodigy by sterile welding and prepared for droplet sorting under a flow hood. Cells were washed with PBS/EDTA supplemented with 0.5% HSA in 50 mL Falcon tubes. After staining with CD95-PE (clone REA738 [Miltenyi Biotec] or clone DX2 [BioLegend, San Diego, CA]) and CD62L-PEVio770 (clone 145/15; Miltenyi Biotec), cells were sorted for $CD95^+CD62L^+$ T_{CM}/T_{SCM} cells using an Aria Fusion II instrument (Becton Dickinson, Heidelberg, Germany) located under a laminar flow hood. Cells were kept at 4°C for the whole sorting procedure. Cells were sorted into HSA-coated tubes containing medium 1, containing additionally 1% penicillin/streptomycin and 1% gentamycin. After the sort, cells were resuspended in an appropriate amount of medium 1 supplemented with 1% penicillin/streptomycin and 1% gentamycin and then reapplied to the TS520 tubing set by sterile welding of a transfer bag. The process was then continued as described for the bulk T cell population. The flow cytometry sort for T_{CM} and T_{SCM} was carried out using a 70 μm nozzle and a maximum flow rate of 18,000 evts/s. To decrease the storage time of sorted cells in sorting buffer, cells were stained and sorted in batches, total processing times for each batch were usually shorter than 2 h. After each batch purification, cells were washed and resuspended in medium 1 supplemented with 1% penicillin/streptomycin and 1% gentamycin. All batches were then combined in a single transfer bag.

Microbiological control

BACTEC bottles (aerobic and anaerobic; BD Biosciences, San Jose, CA) were inoculated at multiple process steps with 500–1,000 μL cellular product obtained from the apheresis material, on day 7 and after the final formulation of the CAR T cells in NaCl with 0.5% HSA, before cryopreservation. Microbiological control was carried out according to European Pharmacopeia (EP) 2.6.27 at the Experimental and Clinical Research Center (ZKP, Charité-University Medicine Berlin, Berlin, Germany) using the BD BACTEC Model 9050.

Flow cytometry

To assess the phenotype of T cells and the composition of the culture, the following primary anti-human antibodies were used (all Miltenyi Biotec, unless otherwise noted): CD45-VioBlue (REA747), CD197-VioBlue (REA546), TIM-3-BV421 (F38-2E2; BioLegend), CD3-BV510 (SK7; BioLegend), CD4-VioGreen (VIT4 or REA623), CD45RA-VioGreen (REA562), CD3-FITC (REA613), CD34-FITC (AC136), CD16-PE (REA423), CD56-PE (REA196), CD69-PE (REA824), CD95-PE (REA738), PD-1-PE (EH12.2H7; BioLegend), CD19-PE-Vio770 (REA675), CD62L-PE-Vio770 (145/15), CD8-PE-Cy7 (HIT8a; BioLegend), CD14-APC (TÜK4 or REA599), CD25-APC (REA945), CD45RO-APC (REA611), LAG-3-AF647 (11C3C65; BioLegend), CD4-APC-Cy7 (OKT4; BioLegend), CD8-APC-Cy7 (HIT8a; BioLegend), and CD8-APC-Vio770 (REA734). As isotype control for REA antibodies REA293 conjugated to

VioBlue, PE, PE-Vio770, or APC was used. Other isotype controls that were used are mouse IgG1k conjugated to BV421, AF647, or PE (MOPC-21; BioLegend). All cell stainings were done in MACSQuant running buffer, without a prior blocking step for Fc receptors. Dead cell discrimination was always included by 7-AAD (Miltenyi Biotech or BioLegend) staining. CAR T cells were detected with either an anti-human IgG1-PE polyclonal goat-anti-human serum (Southern Biotec, Birmingham, AL) or a BCMA-FITC peptide (AcroBiosystems, Newark, DE).

For the quantification of the absolute number of BCMA molecules on the target cell surfaces, QuantiBRITE PE calibration beads were used according to the manufacturer's instructions (BD Bioscience). FACS samples were measured on a MACSQuant 10 flow cytometer (Miltenyi Biotec) and analyzed using FlowJo version 10.5.3 (TreeStar).

Vector copy number determination

Vector copy numbers (VCNs) were determined essentially as described.[28,38] Briefly, genomic DNA of 1×10^6 cells was isolated using a genomic DNA isolation kit (Roboklon, Berlin. Germany), and 100 ng was used to perform qPCR detecting the woodchuck hepatitis virus post-transcriptional regulatory element (WPRE) within the viral insert, normalized to the endogenous polypyrimidine tract binding protein 2 (PTBP2). The primer and probe sequences used were as follows: WPRE: forward: gaggagttgtggcccgttgt, reverse: tgacaggtggtggcaatgcc, probe: FAM-ctgtgtttgctgacgcaac-BHQ1; PTBP2: forward: tctccattccctatcttcatgc, reverse: gttcccgcagaatggtgaggtg, probe: JOE-atgttcctcggaccaacttg-BHQ1 (Eurofins Genomics, Ebersberg, Germany). The reaction was performed using the Applied Biosystems (Foster City, CA) StepOnePlus Real-Time PCR system in triplicate. The conditions were as follows: initially 50°C for 2 min, 95°C for 20 s; 40 cycles of 95°C for 5 s, 56°C for 20 s, and 65°C for 20 s; and primer concentration 330 nM, probe concentration 150 nM, 1× ABI TaqMan Fast Advanced Master Mix (Thermo Fisher Scientific, Waltham, MA). The results were analyzed using StepOne software version 2.2.2 (Thermo Fisher Scientific) and Excel (Microsoft, Redmond, WA). A standard curve was generated by parallel amplification of 10^3–10^6 copies of a linearized standard plasmid (pQPCR-Stdx4). The VCN per transduced cell was normalized to PTBP2 and the transduction rate. The protocol, a reference clone with 1 copy, and the standard plasmid were kindly provided by Dr. Michael Rothe (Hannover Medical School, Germany).

Cell lines

Human multiple myeloma cell lines NCI-H929 and OPM-2 and the B-NHL cell lines DOHH-2 and JeKo-1 (MCL) were obtained from DSMZ (Braunschweig, Germany). The B-ALL cell line REH was obtained from Dr. Stephan Mathas (MDC, Berlin, Germany), and the identity was confirmed by a multiplex cell line authentication test (Multiplexion, Heidelberg, Germany). All cell lines were expanded upon receipt, and aliquots were frozen in liquid nitrogen. The multiple myeloma MM.1S cell line[60] was engineered to express eGFP and luciferase[61] and is termed MM1.S$^{\text{BCMA-high}}$.eGFP in this report. BCMA$^{\text{low}}$-expressing MM1.S cells (MM1.S$^{\text{BCMA-low}}$.eGFP) were recovered from an NSG mouse injected with MM1.S$^{\text{BCMA-high}}$.eGFP cells. After *in vivo* growth, femur from this mouse was flushed, and tumor cells were purified with CD138 microbeads (Miltenyi Biotec) and expanded, and stocks were frozen in liquid nitrogen. The level of surface-deposited BCMA was determined using FACS analysis. eGFP-expressing cell lines (JeKo-1.eGFP, DOHH-2.eGFP, and RE-H.eGFP) were generated by lentiviral transduction,[28] exactly as described. Cell stocks were stored in liquid nitrogen. All human suspension cell lines were cultured in RPMI 1640 + L-glutamine (Thermo Fisher Scientific) containing 10% fetal calf serum (FCS) (Thermo Fisher Scientific or PAN-Biotech), 1% penicillin/streptomycin, 1% non-essential amino acids, and 1% sodium pyruvate (Thermo Fisher Scientific).

In vitro cytotoxicity assay

A standard [^{51}Cr]-chromium release cytotoxicity assay was applied. BCMA CAR T cells were thawed and cultured overnight in human T cell medium (hTCM + 15% FCS) containing RPMI 1640 + L-glutamine, 15% FCS, 1% penicillin/streptomycin, 1% non-essential amino acids, and 1% sodium pyruvate, supplemented with 0.1 ng/mL IL-7 and 0.1 ng/mL IL-15 (both premium grade; Miltenyi Biotec). The following day, target cells were labeled with 20 μCi [^{51}Cr] sodium chromate (PerkinElmer, Waltham, MA) for 90 min at 37°C. After washing, 2×10^3 target cells were co-cultured in 96-well plates for 4 h at 37°C with CAR T cells at different effector-to-target (E/T) cell ratios. Spontaneous release was determined from target cell supernatant without CAR T cells. Maximum release was assessed using target cell lysis induced by air drying. Cell-free supernatants were harvested and transferred to LUMA-scintillation plates and air-dried, and the released [^{51}Cr] was assessed using a Top γ-Scintillation Count Reader (PerkinElmer). Samples were run in triplicate. Specific lysis was calculated as percentage lysis = (experimental lysis − spontaneous release) × 100/(maximum lysis − spontaneous release).

Additionally, a FACS-based *in vitro* cytotoxicity assay was used. CAR T cells were thawed and cultured in hTCM + 10% FCS with the addition of 10 ng/mL IL-7, 10 ng/mL IL-15, 10 IU/mL IL-2 (all Miltenyi Biotec, premium grade), and 5 μL/mL TransAct beads for 4 days. T cells were then washed, counted, adjusted to the amount of CAR$^+$ T cells, and seeded at the indicated effector to target cell ratios with 5×10^4 GFP$^+$ target cells. The number of remaining viable (7-AAD$^-$) GFP$^+$ tumor cells was determined after 24 h on a MACSQuant 10 flow cytometer and analyzed with FlowJo version 10.5.3. Killing was determined by normalization to the number of tumor cells grown without CAR T cells.

Cytokine-release assay

BCMA CAR T cells (5×10^4) were thawed and co-cultured at a 1:1 ratio with target cells (BCMA$^+$ JeKo-1 and DOHH-2) and control cells (BCMA$^-$ REH) in hTCM + 10% FCS. After 22 h, cell-free supernatants were harvested and stored at −20°C till cytokine analysis. The concentrations of IFN-γ, IL-2, and TNF-α were measured using ELISA (BD Biosciences) according to the manufacturer's instructions. Spontaneous release (min) was assessed by T cell culture without

target cells, and maximal release was induced by stimulation of T cells with 1 μg/mL phorbol-12-myristate-13-acetate (PMA) and 50 μM ionomycin (both Sigma-Aldrich/Merck).

Repetitive antigen stimulation assay

This assay was performed essentially as described.[28,38] Briefly, thawed BCMA CAR T cells were co-cultured in a 1:1 ratio with MM1.S$^{BCMA\text{-}high}$-eGFP$^+$ target cells (5×10^5 cells each per well of a 24-well plate) in hTCM + 10% FCS, in the presence of 0.1 ng/mL IL-7 and 0.1 ng/mL IL-15. After 72 h, cell-free supernatant was harvested and stored frozen until analysis. IFN-γ secretion was quantified using ELISA as described above. Cells were then thoroughly resuspended, and an aliquot was used for counting and flow cytometric analysis of remaining target cells (viable 7-AAD$^-$GFP$^+$CD3$^-$). After calculation of the remaining viable 7-AAD$^-$T cells, T cells were again seeded at a 1:1 ratio with fresh MM1.S$^{BCMA\text{-}high}$-eGFP$^+$ target cells in new 24-well plates. Cells were analyzed after each round of 72 h for the same parameters.

For the analysis of isolated CD8$^+$ CAR T cells in the repetitive antigen assay, BCMA CAR T cells were thawed and cultured in hTCM + 10% FCS with the addition of 10 ng/mL IL-7, 10 ng/mL IL-15, 10 IU/mL IL-2 (premium grade), and 5 μL/mL TransAct beads for 5 days. CD8$^+$ T cells were then isolated using the human CD8$^+$ T cell isolation kit according to the manufacturer's recommendations (Miltenyi Biotec) and subsequently used for the repetitive antigen stimulation assay as aforementioned. For the repetitive stimulation of CD8$^+$ CAR T cells, 1 ng/mL IL-7, 1 ng/mL IL-15, and 10 IU/mL IL-2 were used to supplement hTCM + 10% FCS.

Quantitative real-time PCR analysis

RNA was isolated from the MACS and HARV products of runs P1–P4 using the RNeasy Mini Kit (Qiagen, Hilden, Germany). RNA was transcribed into cDNA using the SuperScript VILO cDNA Synthesis kit (Thermo Fisher Scientific). Quantitative real-time PCR analysis was performed using TaqMan Gene Expression Assays for TCF7, BCL2, LEF1, ID3, TBX21, EOMES, PRDM1, IFNG, GZMB, and B2M (Thermo Fisher Scientific) and the TaqMan Fast Advanced Master Mix (Thermo Fisher Scientific). Reactions were performed in duplicate using the Applied Biosystems StepOnePlus Real-Time PCR system. Results were analyzed using StepOne software (version 2.2.2) and Excel. Relative gene expression was calculated using the ΔΔCt method by first normalizing each sample to the expression of the housekeeping gene B2M (ΔCt) and then by normalizing each CAR T cell HARV sample to its respective MACS sample (ΔΔCt).

Statistical analysis

Results are expressed as arithmetic mean ± SEM if not otherwise stated. For each run, each sample was measured in technical replicate.

Values of $p < 0.05$ were considered to indicate statistical significance, as determined using the Mann-Whitney U test, as appropriate. Analyses were performed using Prism versions 6.0 and 9.0 (GraphPad Software).

SUPPLEMENTAL INFORMATION

Supplemental information can be found online at https://doi.org/10.1016/j.omtm.2021.12.005.

ACKNOWLEDGMENTS

We thank Vivien Kretschmer (MDC, Berlin) for excellent technical assistance. We further acknowledge Dr. Martin Vaegler from the Experimental and Clinical Research Center (ECRC), Charité-University Medicine Berlin, Berlin, Germany, for performing microbiological assays. We thank the team of the Stem Cell Facility at the Charité-University Medicine Berlin, Clinic for Hematology, Oncology and Tumorimmunology (Berlin, Germany) for support in leukapheresis. This work was funded by the Helmholtz Validation Fond (HVF#0057) and in part by a VIP$^+$ BMBF grant (03VP05030) awarded to A.R. and U.E.H.

AUTHOR CONTRIBUTIONS

Conception and Design, J.J.J. and A.R.; Development of Methodology, J.J.J., U.G., A.K., and A.R.; Acquisition of Data, J.J.J., U.G., and K.G.; Analysis and Interpretation of Data, J.J.J., U.G., U.E.H., and A.R.; Writing, Review, and/or Revision of the Manuscript, J.J.J., U.E.H., A.K., U.G., and A.R.; Study Supervision: A.R. and U.E.H. All authors reviewed the manuscript.

DECLARATION OF INTERESTS

U.E.H. and A.R. have filed a patent application for the BCMA CAR (WO 2017211900A1). The authors declared no competing interests regarding data acquisition and interpretation. A.R. and U.E.H. have received research funding from Fate Therapeutics (San Diego, CA) for work unrelated to the main topic of this report.

REFERENCES

1. Maude, S.L., Laetsch, T.W., Buechner, J., Rives, S., Boyer, M., Bittencourt, H., Bader, P., Verneris, M.R., Stefanski, H.E., Myers, G.D., et al. (2018). Tisagenlecleucel in children and young adults with B-cell lymphoblastic leukemia. N. Engl. J. Med. *378*, 439–448. https://doi.org/10.1056/NEJMoa1709866.

2. June, C.H., O'Connor, R.S., Kawalekar, O.U., Ghassemi, S., and Milone, M.C. (2018). CAR T cell immunotherapy for human cancer. Science *359*, 1361–1365. https://doi.org/10.1126/science.aar6711.

3. Neelapu, S.S., Locke, F.L., Bartlett, N.L., Lekakis, L.J., Miklos, D.B., Jacobson, C.A., Braunschweig, I., Oluwole, O.O., Siddiqi, T., Lin, Y., et al. (2017). Axicabtagene ciloleucel CAR T-cell therapy in refractory large B-cell lymphoma. N. Engl. J. Med. *377*, 2531–2544. https://doi.org/10.1056/NEJMoa1707447.

4. Park, J.H., Riviere, I., Gonen, M., Wang, X., Senechal, B., Curran, K.J., Sauter, C., Wang, Y., Santomasso, B., Mead, E., et al. (2018). Long-term follow-up of CD19 CAR therapy in acute lymphoblastic leukemia. N. Engl. J. Med. *378*, 449–459. https://doi.org/10.1056/NEJMoa1709919.

5. Raje, N., Berdeja, J., Lin, Y., Siegel, D., Jagannath, S., Madduri, D., Liedtke, M., Rosenblatt, J., Maus, M.V., Turka, A., et al. (2019). Anti-BCMA CAR T-cell therapy bb2121 in relapsed or refractory multiple myeloma. N. Engl. J. Med. *380*, 1726–1737. https://doi.org/10.1056/NEJMoa1817226.

6. Brudno, J.N., Maric, I., Hartman, S.D., Rose, J.J., Wang, M., Lam, N., Stetler-Stevenson, M., Salem, D., Yuan, C., Pavletic, S., et al. (2018). T cells genetically modified to express an anti-B-cell maturation antigen chimeric antigen receptor cause remissions of poor-prognosis relapsed multiple myeloma. J. Clin. Oncol. *36*, 2267–2280. https://doi.org/10.1200/JCO.2018.77.8084.

7. Arcangeli, S., Falcone, L., Camisa, B., De Girardi, F., Biondi, M., Giglio, F., Ciceri, F., Bonini, C., Bondanza, A., and Casucci, M. (2020). Next-generation manufacturing protocols enriching TSCM CAR T cells can overcome disease-specific T cell defects in cancer patients. Front. Immunol. *11*, 1217. https://doi.org/10.3389/fimmu.2020.01217.

8. Blaeschke, F., Stenger, D., Kaeuferle, T., Willier, S., Lotfi, R., Kaiser, A.D., Assenmacher, M., Doring, M., Feucht, J., and Feuchtinger, T. (2018). Induction of a central memory and stem cell memory phenotype in functionally active CD4(+) and CD8(+) CAR T cells produced in an automated good manufacturing practice system for the treatment of CD19(+) acute lymphoblastic leukemia. Cancer Immunol. Immunother. *67*, 1053–1066. https://doi.org/10.1007/s00262-018-2155-7.

9. Sabatino, M., Hu, J., Sommariva, M., Gautam, S., Fellowes, V., Hocker, J.D., Dougherty, S., Qin, H., Klebanoff, C.A., Fry, T.J., et al. (2016). Generation of clinical-grade CD19-specific CAR-modified CD8+ memory stem cells for the treatment of human B-cell malignancies. Blood *128*, 519–528. https://doi.org/10.1182/blood-2015-11-683847.

10. Xu, Y., Zhang, M., Ramos, C.A., Durett, A., Liu, E., Dakhova, O., Liu, H., Creighton, C.J., Gee, A.P., Heslop, H.E., et al. (2014). Closely related T-memory stem cells correlate with in vivo expansion of CAR.CD19-T cells and are preserved by IL-7 and IL-15. Blood *123*, 3750–3759. https://doi.org/10.1182/blood-2014-01-552174.

11. Wang, X., Naranjo, A., Brown, C.E., Bautista, C., Wong, C.W., Chang, W.C., Aguilar, B., Ostberg, J.R., Riddell, S.R., Forman, S.J., and Jensen, M.C. (2012). Phenotypic and functional attributes of lentivirus-modified CD19-specific human CD8+ central memory T cells manufactured at clinical scale. J. Immunother. *35*, 689–701. https://doi.org/10.1097/CJI.0b013e318270dec7.

12. Wang, X., Popplewell, L.L., Wagner, J.R., Naranjo, A., Blanchard, M.S., Mott, M.R., Norris, A.P., Wong, C.W., Urak, R.Z., Chang, W.C., et al. (2016). Phase 1 studies of central memory-derived CD19 CAR T-cell therapy following autologous HSCT in patients with B-cell NHL. Blood *127*, 2980–2990. https://doi.org/10.1182/blood-2015-12-686725.

13. Louis, C.U., Savoldo, B., Dotti, G., Pule, M., Yvon, E., Myers, G.D., Rossig, C., Russell, H.V., Diouf, O., Liu, E., et al. (2011). Antitumor activity and long-term fate of chimeric antigen receptor-positive T cells in patients with neuroblastoma. Blood *118*, 6050–6056. https://doi.org/10.1182/blood-2011-05-354449.

14. Castella, M., Caballero-Banos, M., Ortiz-Maldonado, V., Gonzalez-Navarro, E.A., Sune, G., Antonana-Vidosola, A., Boronat, A., Marzal, B., Millan, L., Martin-Antonio, B., et al. (2020). Point-of-care CAR T-cell production (ARI-0001) using a closed semi-automatic bioreactor: experience from an academic phase I clinical trial. Front. Immunol. *11*, 482. https://doi.org/10.3389/fimmu.2020.00482.

15. Priesner, C., Aleksandrova, K., Esser, R., Mockel-Tenbrinck, N., Leise, J., Drechsel, K., Marburger, M., Quaiser, A., Goudeva, L., Arseniev, L., et al. (2016). Automated enrichment, transduction, and expansion of clinical-scale CD62L(+) T cells for manufacturing of gene therapy medicinal products. Hum. Gene Ther. *27*, 860–869. https://doi.org/10.1089/hum.2016.091.

16. Casati, A., Varghaei-Nahvi, A., Feldman, S.A., Assenmacher, M., Rosenberg, S.A., Dudley, M.E., and Scheffold, A. (2013). Clinical-scale selection and viral transduction of human naive and central memory CD8+ T cells for adoptive cell therapy of cancer patients. Cancer Immunol. Immunother. *62*, 1563–1573. https://doi.org/10.1007/s00262-013-1459-x.

17. Mock, U., Nickolay, L., Philip, B., Cheung, G.W., Zhan, H., Johnston, I.C.D., Kaiser, A.D., Peggs, K., Pule, M., Thrasher, A.J., and Qasim, W. (2016). Automated manufacturing of chimeric antigen receptor T cells for adoptive immunotherapy using CliniMACS Prodigy. Cytotherapy *18*, 1002–1011. https://doi.org/10.1016/j.jcyt.2016.05.009.

18. Lock, D., Mockel-Tenbrinck, N., Drechsel, K., Barth, C., Mauer, D., Schaser, T., Kolbe, C., Al Rawashdeh, W., Brauner, J., Hardt, O., et al. (2017). Automated manufacturing of potent CD20-directed chimeric antigen receptor T cells for clinical use. Hum. Gene Ther. *28*, 914–925. https://doi.org/10.1089/hum.2017.111.

19. Zhu, F., Shah, N., Xu, H., Schneider, D., Orentas, R., Dropulic, B., Hari, P., and Keever-Taylor, C.A. (2018). Closed-system manufacturing of CD19 and dual-targeted CD20/19 chimeric antigen receptor T cells using the CliniMACS Prodigy device at an academic medical center. Cytotherapy *20*, 394–406. https://doi.org/10.1016/j.jcyt.2017.09.005.

20. Castella, M., Boronat, A., Martin-Ibanez, R., Rodriguez, V., Sune, G., Caballero, M., Marzal, B., Perez-Amill, L., Martin-Antonio, B., Castano, J., et al. (2019). Development of a novel anti-CD19 chimeric antigen receptor: a paradigm for an affordable CAR T cell production at academic institutions. Mol. Ther. Methods Clin. Dev. *12*, 134–144. https://doi.org/10.1016/j.omtm.2018.11.010.

21. Zhang, W., Jordan, K.R., Schulte, B., and Purev, E. (2018). Characterization of clinical grade CD19 chimeric antigen receptor T cells produced using automated CliniMACS Prodigy system. Drug Des. Devel Ther. *12*, 3343–3356. https://doi.org/10.2147/DDDT.S175113.

22. Aleksandrova, K., Leise, J., Priesner, C., Melk, A., Kubaink, F., Abken, H., Hombach, A., Aktas, M., Essl, M., Burger, I., et al. (2019). Functionality and cell senescence of CD4/CD8-selected CD20 CAR T cells manufactured using the automated CliniMACS Prodigy(R) platform. Transfus. Med. Hemother *46*, 47–54. https://doi.org/10.1159/000495772.

23. Fernandez, L., Fernandez, A., Mirones, I., Escudero, A., Cardoso, L., Vela, M., Lanzarot, D., de Paz, R., Leivas, A., Gallardo, M., et al. (2019). GMP-compliant manufacturing of NKG2D CAR memory T cells using CliniMACS Prodigy. Front. Immunol. *10*, 2361. https://doi.org/10.3389/fimmu.2019.02361.

24. Vedvyas, Y., McCloskey, J.E., Yang, Y., Min, I.M., Fahey, T.J., Zarnegar, R., Hsu, Y.S., Hsu, J.M., Van Besien, K., Gaudet, I., et al. (2019). Manufacturing and preclinical validation of CAR T cells targeting ICAM-1 for advanced thyroid cancer therapy. Sci. Rep. *9*, 10634. https://doi.org/10.1038/s41598-019-46938-7.

25. Perez-Amill, L., Sune, G., Antonana-Vildosola, A., Castella, M., Najjar, A., Bonet, J., Fernandez-Fuentes, N., Inoges, S., Lopez, A., Bueno, C., et al. (2021). Preclinical development of a humanized chimeric antigen receptor against B cell maturation antigen for multiple myeloma. Haematologica *106*, 173–184. https://doi.org/10.3324/haematol.2019.228577.

26. Brentjens, R.J., Riviere, I., Park, J.H., Davila, M.L., Wang, X., Stefanski, J., Taylor, C., Yeh, R., Bartido, S., Borquez-Ojeda, O., et al. (2011). Safety and persistence of adoptively transferred autologous CD19-targeted T cells in patients with relapsed or chemotherapy refractory B-cell leukemias. Blood *118*, 4817–4828. https://doi.org/10.1182/blood-2011-04-348540.

27. Davila, M.L., Riviere, I., Wang, X., Bartido, S., Park, J., Curran, K., Chung, S.S., Stefanski, J., Borquez-Ojeda, O., Olszewska, M., et al. (2014). Efficacy and toxicity management of 19-28z CAR T cell therapy in B cell acute lymphoblastic leukemia. Sci. Transl. Med. *6*, 224ra225. https://doi.org/10.1126/scitranslmed.3008226.

28. Bluhm, J., Kieback, E., Marino, S.F., Oden, F., Westermann, J., Chmielewski, M., Abken, H., Uckert, W., Hopken, U.E., and Rehm, A. (2018). CAR T cells with enhanced sensitivity to B cell maturation antigen for the targeting of B cell non-Hodgkin's lymphoma and multiple myeloma. Mol. Ther. *26*, 1906–1920. https://doi.org/10.1016/j.ymthe.2018.06.012.

29. Kustikova, O.S., Geiger, H., Li, Z., Brugman, M.H., Chambers, S.M., Shaw, C.A., Pike-Overzet, K., de Ridder, D., Staal, F.J., von Keudell, G., et al. (2007). Retroviral vector insertion sites associated with dominant hematopoietic clones mark "stemness" pathways. Blood *109*, 1897–1907. https://doi.org/10.1182/blood-2006-08-044156.

30. Banerjee, P., Crawford, L., Samuelson, E., and Feuer, G. (2010). Hematopoietic stem cells and retroviral infection. Retrovirology *7*, 8. https://doi.org/10.1186/1742-4690-7-8.

31. Sutherland, D.R., Anderson, L., Keeney, M., Nayar, R., and Chin-Yee, I. (1996). The ISHAGE guidelines for CD34+ cell determination by flow cytometry. International Society of Hematotherapy and Graft Engineering. J. Hematother *5*, 213–226. https://doi.org/10.1089/scd.1.1996.5.213.

32. Keeney, M., Chin-Yee, I., Weir, K., Popma, J., Nayar, R., and Sutherland, D.R. (1998). Single platform flow cytometric absolute CD34+ cell counts based on the ISHAGE guidelines. International Society of Hematotherapy and Graft Engineering. Cytometry *34*, 61–70.

33. Gattinoni, L., Klebanoff, C.A., and Restifo, N.P. (2009). Pharmacologic induction of CD8+ T cell memory: better living through chemistry. Sci. Transl Med. *1*, 11ps12. https://doi.org/10.1126/scitranslmed.3000302.

34. Gattinoni, L., Zhong, X.S., Palmer, D.C., Ji, Y., Hinrichs, C.S., Yu, Z., Wrzesinski, C., Boni, A., Cassard, L., Garvin, L.M., et al. (2009). Wnt signaling arrests effector T cell differentiation and generates CD8+ memory stem cells. Nat. Med. *15*, 808–813. https://doi.org/10.1038/nm.1982.

35. Gattinoni, L., Ji, Y., and Restifo, N.P. (2010). Wnt/beta-catenin signaling in T-cell immunity and cancer immunotherapy. Clin. Cancer Res. *16*, 4695–4701. https://doi.org/10.1158/1078-0432.CCR-10-0356.

36. Kaneko, S., Mastaglio, S., Bondanza, A., Ponzoni, M., Sanvito, F., Aldrighetti, L., Radrizzani, M., La Seta-Catamancio, S., Provasi, E., Mondino, A., et al. (2009). IL-7 and IL-15 allow the generation of suicide gene-modified alloreactive self-renewing central memory human T lymphocytes. Blood *113*, 1006–1015. https://doi.org/10.1182/blood-2008-05-156059.

37. Cieri, N., Camisa, B., Cocchiarella, F., Forcato, M., Oliveira, G., Provasi, E., Bondanza, A., Bordignon, C., Peccatori, J., Ciceri, F., et al. (2013). IL-7 and IL-15 instruct the generation of human memory stem T cells from naive precursors. Blood *121*, 573–584. https://doi.org/10.1182/blood-2012-05-431718.

38. Bunse, M., Pfeilschifter, J., Bluhm, J., Zschummel, M., Joedicke, J.J., Wirges, A., Stark, H., Kretschmer, V., Chmielewski, M., Uckert, W., et al. (2021). CXCR5 CAR-T cells simultaneously target B cell non-Hodgkin's lymphoma and tumor-supportive follicular T helper cells. Nat. Commun. *12*, 240. https://doi.org/10.1038/s41467-020-20488-3.

39. Sommermeyer, D., Hudecek, M., Kosasih, P.L., Gogishvili, T., Maloney, D.G., Turtle, C.J., and Riddell, S.R. (2016). Chimeric antigen receptor-modified T cells derived from defined CD8+ and CD4+ subsets confer superior antitumor reactivity in vivo. Leukemia *30*, 492–500. https://doi.org/10.1038/leu.2015.247.

40. Zhao, D.M., Yu, S., Zhou, X., Haring, J.S., Held, W., Badovinac, V.P., Harty, J.T., and Xue, H.H. (2010). Constitutive activation of Wnt signaling favors generation of memory CD8 T cells. J. Immunol. *184*, 1191–1199. https://doi.org/10.4049/jimmunol.0901199.

41. Zhou, X., and Xue, H.H. (2012). Cutting edge: generation of memory precursors and functional memory CD8+ T cells depends on T cell factor-1 and lymphoid enhancer-binding factor-1. J. Immunol. *189*, 2722–2726. https://doi.org/10.4049/jimmunol.1201150.

42. Klaver, Y., van Steenbergen, S.C., Sleijfer, S., Debets, R., and Lamers, C.H. (2016). T cell maturation stage prior to and during GMP processing informs on CAR T cell expansion in patients. Front. Immunol. *7*, 648. https://doi.org/10.3389/fimmu.2016.00648.

43. Oliveira, G., Ruggiero, E., Stanghellini, M.T., Cieri, N., D'Agostino, M., Fronza, R., Lulay, C., Dionisio, F., Mastaglio, S., Greco, R., et al. (2015). Tracking genetically engineered lymphocytes long-term reveals the dynamics of T cell immunological memory. Sci. Transl. Med. *7*, 317ra198. https://doi.org/10.1126/scitranslmed.aac8265.

44. Kondo, T., Imura, Y., Chikuma, S., Hibino, S., Omata-Mise, S., Ando, M., Akanuma, T., Iizuka, M., Sakai, R., Morita, R., and Yoshimura, A. (2018). Generation and application of human induced-stem cell memory T cells for adoptive immunotherapy. Cancer Sci. *109*, 2130–2140. https://doi.org/10.1111/cas.13648.

45. Gattinoni, L., Klebanoff, C.A., Palmer, D.C., Wrzesinski, C., Kerstann, K., Yu, Z., Finkelstein, S.E., Theoret, M.R., Rosenberg, S.A., and Restifo, N.P. (2005). Acquisition of full effector function in vitro paradoxically impairs the in vivo antitumor efficacy of adoptively transferred CD8+ T cells. J. Clin. Invest. *115*, 1616–1626. https://doi.org/10.1172/JCI24480.

46. Gattinoni, L., Lugli, E., Ji, Y., Pos, Z., Paulos, C.M., Quigley, M.F., Almeida, J.R., Gostick, E., Yu, Z., Carpenito, C., et al. (2011). A human memory T cell subset with stem cell-like properties. Nat. Med. *17*, 1290–1297. https://doi.org/10.1038/nm.2446.

47. Kaech, S.M., and Cui, W. (2012). Transcriptional control of effector and memory CD8+ T cell differentiation. Nat. Rev. Immunol. *12*, 749–761. https://doi.org/10.1038/nri3307.

48. Szabo, S.J., Sullivan, B.M., Stemmann, C., Satoskar, A.R., Sleckman, B.P., and Glimcher, L.H. (2002). Distinct effects of T-bet in TH1 lineage commitment and IFN-gamma production in CD4 and CD8 T cells. Science *295*, 338–342. https://doi.org/10.1126/science.1065543.

49. Szabo, S.J., Kim, S.T., Costa, G.L., Zhang, X., Fathman, C.G., and Glimcher, L.H. (2000). A novel transcription factor, T-bet, directs Th1 lineage commitment. Cell *100*, 655–669. https://doi.org/10.1016/s0092-8674(00)80702-3.

50. Intlekofer, A.M., Takemoto, N., Wherry, E.J., Longworth, S.A., Northrup, J.T., Palanivel, V.R., Mullen, A.C., Gasink, C.R., Kaech, S.M., Miller, J.D., et al. (2005). Effector and memory CD8+ T cell fate coupled by T-bet and eomesodermin. Nat. Immunol. *6*, 1236–1244. https://doi.org/10.1038/ni1268.

51. McLane, L.M., Banerjee, P.P., Cosma, G.L., Makedonas, G., Wherry, E.J., Orange, J.S., and Betts, M.R. (2013). Differential localization of T-bet and Eomes in CD8 T cell memory populations. J. Immunol. *190*, 3207–3215. https://doi.org/10.4049/jimmunol.1201556.

52. de Araujo-Souza, P.S., Hanschke, S.C., and Viola, J.P. (2015). Epigenetic control of interferon-gamma expression in CD8 T cells. J. Immunol. Res. *2015*, 849573. https://doi.org/10.1155/2015/849573.

53. Balasubramani, A., Mukasa, R., Hatton, R.D., and Weaver, C.T. (2010). Regulation of the Ifng locus in the context of T-lineage specification and plasticity. Immunol. Rev. *238*, 216–232. https://doi.org/10.1111/j.1600-065X.2010.00961.x.

54. Zhao, Z., Condomines, M., van der Stegen, S.J.C., Perna, F., Kloss, C.C., Gunset, G., Plotkin, J., and Sadelain, M. (2015). Structural design of engineered costimulation determines tumor rejection kinetics and persistence of CAR T cells. Cancer Cell *28*, 415–428. https://doi.org/10.1016/j.ccell.2015.09.004.

55. Golumba-Nagy, V., Kuehle, J., Hombach, A.A., and Abken, H. (2018). CD28-zeta CAR T cells resist TGF-beta repression through IL-2 signaling, which can be mimicked by an engineered IL-7 autocrine loop. Mol. Ther. *26*, 2218–2230. https://doi.org/10.1016/j.ymthe.2018.07.005.

56. Kawalekar, O.U., O'Connor, R.S., Fraietta, J.A., Guo, L., McGettigan, S.E., Posey, A.D., Jr., Patel, P.R., Guedan, S., Scholler, J., Keith, B., et al. (2016). Distinct signaling of coreceptors regulates specific metabolism pathways and impacts memory development in CAR T cells. Immunity *44*, 380–390. https://doi.org/10.1016/j.immuni.2016.01.021.

57. Abken, H. (2016). Costimulation engages the gear in driving CARs. Immunity *44*, 214–216. https://doi.org/10.1016/j.immuni.2016.02.001.

58. Hennig, K., Raasch, L., Kolbe, C., Weidner, S., Leisegang, M., Uckert, W., Titeux, M., Hovnanian, A., Kuehlcke, K., and Loew, R. (2014). HEK293-based production platform for gamma-retroviral (self-inactivating) vectors: application for safe and efficient transfer of COL7A1 cDNA. Hum. Gene Ther. Clin. Dev. *25*, 218–228. https://doi.org/10.1089/humc.2014.083.

59. Wang, X., Olszewska, M., Qu, J., Wasielewska, T., Bartido, S., Hermetet, G., Sadelain, M., and Riviere, I. (2015). Large-scale clinical-grade retroviral vector production in a fixed-bed bioreactor. J. Immunother. *38*, 127–135. https://doi.org/10.1097/CJI.0000000000000072.

60. Greenstein, S., Krett, N.L., Kurosawa, Y., Ma, C., Chauhan, D., Hideshima, T., Anderson, K.C., and Rosen, S.T. (2003). Characterization of the MM.1 human multiple myeloma (MM) cell lines: a model system to elucidate the characteristics, behavior, and signaling of steroid-sensitive and -resistant MM cells. Exp. Hematol. *31*, 271–282. https://doi.org/10.1016/s0301-472x(03)00023-7.

61. Oden, F., Marino, S.F., Brand, J., Scheu, S., Kriegel, C., Olal, D., Takvorian, A., Westermann, J., Yilmaz, B., Hinz, M., et al. (2015). Potent anti-tumor response by targeting B cell maturation antigen (BCMA) in a mouse model of multiple myeloma. Mol. Oncol. *9*, 1348–1358. https://doi.org/10.1016/j.molonc.2015.03.010.